Revised Version

DESY 03-024
HIP-2002-57/TH
FTUAM 03/05
IFT-UAM/CSIC-03-09

DESY 03-024
HIP-2002-57/TH
FTUAM 03/05
IFT-UAM/CSIC-03-09
hep-ph/0304115
April 2003

Neutralino-Nucleon Cross Section and Charge and Colour Breaking Constraints

D.G. Cerdeño[1], E. Gabrielli[2], M.E. Gomez[3], C. Muñoz[4]

[1] *II. Institut für Theoretische Physik, Universität Hamburg, Luruper Chaussee 149, D-22761 Hamburg, Germany.*

[2] *Helsinki Institute of Physics, P.O. Box 64, FIN-00014 Helsinki, Finland.*

[3] *Departamento de Física and Grupo Teórico de Física de Partículas, Instituto Superior Técnico, Av. Rovisco Pais, 1049-001 Lisboa, Portugal*

[4] *Departamento de Física Teórica C-XI and Instituto de Física Teórica C-XVI, Universidad Autónoma de Madrid, Cantoblanco, 28049 Madrid, Spain.*

arXiv:hep-ph/0304115 v3 30 Jun 2003

Abstract

We compute the neutralino-nucleon cross section in several supersymmetric scenarios, taking into account all kind of constraints. In particular, the constraints that the absence of dangerous charge and colour breaking minima imposes on the parameter space are studied in detail. In addition, the most recent experimental constraints, such as the lower bound on the Higgs mass, the $b \to s\gamma$ branching ratio, and the muon $g-2$ are considered. The astrophysical bounds on the dark matter density are also imposed on the theoretical computation of the relic neutralino density, assuming thermal production. This computation is relevant for the theoretical analysis of the direct detection of dark matter in current experiments. We consider first the supergravity scenario with universal soft terms and GUT scale. In this scenario the charge and colour breaking constraints turn out to be quite important, and $\tan\beta \lesssim 20$ is forbidden. Larger values of $\tan\beta$ can also be forbidden, depending on the value of the trilinear parameter A. Finally, we study supergravity scenarios with an intermediate scale, and also with non-universal scalar and gaugino masses where the cross section can be very large.

1 Introduction

A weakly-interacting massive particle (WIMP) is one of the most interesting candidates for the dark matter in the Universe. Since WIMPs would cluster gravitationally with ordinary stars in the galactic halos, there is the hope of detecting relic WIMPs directly, by observing their elastic scattering on target nuclei through nuclear recoils [1]. In fact, one of the current experiments, the DAMA collaboration, has reported data favouring the existence of a WIMP signal [2]. It was claimed that the preferred range of the WIMP-nucleon cross section is $10^{-6} - 10^{-5}$ pb for a WIMP mass between 30 and 270 GeV [2, 3]. Unlike this spectacular result, other collaborations such as CDMS [4], EDELWEISS [5], IGEX [6], and ZEPLIN I [7] claim to have excluded important regions of the DAMA parameter space.

In any case, due to these and other projected experiments, it seems very plausible that the dark matter will be found in the near future. In this situation, and assuming that the dark matter is a WIMP, it is natural to wonder how big the cross section for its direct detection can be. The answer to this question depends on the particular WIMP considered. The leading candidate in this class is the lightest neutralino [1], $\tilde{\chi}_1^0$, a particle predicted by the supersymmetric (SUSY) extension of the standard model (SM).

In this paper we will analyse the SUSY scenario in the framework of supergravity (SUGRA). Working in this framework one makes several assumptions. In particular, the soft parameters, i.e., gaugino masses, scalar masses, and trilinear couplings, are generated once SUSY is broken through gravitational interactions. They are denoted at the grand unification scale ($M_{GUT} \approx 2 \times 10^{16}$ GeV) by M_a, m_α, and $A_{\alpha\beta\gamma}$, respectively. Likewise, radiative electroweak symmetry breaking is imposed, and one loop renormalization group equations (RGEs) are used to derive low-energy SUSY parameters. Let us also recall that the Higgsino mass parameter μ is determined by the minimization of the Higgs effective potential. This implies

$$\mu^2 = \frac{m_{H_d}^2 - m_{H_u}^2 \tan^2\beta}{\tan^2\beta - 1} - \frac{1}{2} M_Z^2 \ , \tag{1}$$

where $\tan\beta = \langle H_u^0 \rangle / \langle H_d^0 \rangle$ is the ratio of Higgs vacuum expectation values. The effect of the one-loop corrections to the scalar potential can be minimized by evaluating the μ term at the scale $M_{SUSY} = \sqrt{m_{\tilde{t}_1} m_{\tilde{t}_2}}$ [8, 9].

With these assumptions, the SUGRA framework still allows a large number of free parameters. In order to have predictive power one usually assumes that the above soft parameters are universal at M_{GUT}. This is the so-called minimal supergravity (mSUGRA) scenario, where there are only four free parameters: m, M, A, and $\tan\beta$. In addition, the sign of μ remains also undetermined. It is worth noticing that explicit string constructions with these characteristics can be found [10]. In any case, the general situation for the soft parameters in supergravity is to have a non-universal structure [10]. For the case of the observable scalar masses this is due to the non-universal couplings in the Kähler potential between the hidden sector fields breaking SUSY and the observable sector fields. For the case of the gaugino masses this is due

to the non-universality of the gauge kinetic functions associated to the different gauge groups. Of course, general string constructions, whose low-energy limit is SUGRA, exhibit these properties [10].

Although the cross section for the elastic scattering of $\tilde{\chi}_1^0$ on nucleons in the mSUGRA and non-universal SUGRA frameworks has been examined exhaustively in the literature (for recent works see e.g. refs. [11]-[21]), no analyses can be found concerning the constraints that arise from imposing the absence of charge and colour breaking minima. This is the aim of the present paper.

As is well known, the presence of scalar fields with colour and electric charge in SUSY theories induces the possible existence of dangerous charge and colour breaking minima, which would make the standard vacuum unstable [22]-[30]. The presence of these instabilities may imply either that the corresponding model is inconsistent or that it requires non-trivial cosmology to justify that the Universe eventually fell in the phenomenologically realistic (but local) minimum [22, 31]. The constraints on the parameter space of the theory that arise from imposing the absence of these instabilities are very important [24], and we will study their consequences on the neutralino-nucleon cross section.

The paper is organized as follows. In Section 2 we will briefly review the potentially dangerous charge and colour breaking directions in the field space of SUGRA and how to avoid them. On the other hand, a correct phenomenology is also essential in our analysis of the neutralino-nucleon cross section, and we will discuss in Section 3 the most recent experimental and astrophysical constraints which can affect this computation. Then, in the rest of the paper, we will re-evaluate the cross section taking into account the charge and colour breaking constraints in addition to the experimental and astrophysical ones. In particular, in Section 4 we will study the value of the cross section when the mSUGRA scenario is considered. First, we will analyse this scenario in the usual context of a GUT scale, $M_{GUT} \approx 2 \times 10^{16}$ GeV, and second we will discuss how these results are modified when the GUT condition is relaxed. In particular, we will consider the case of an intermediate scale. Finally, in Section 5, the most general situation in the context of SUGRA, non-universal scalar and gaugino masses, will be studied. These analyses have been carried out for different values of the trilinear parameter A. The conclusions are left for Section 6.

2 Charge and colour breaking constraints

The basic ingredient of our analysis concerns the constraints associated with the existence of dangerous directions in the field space. A complete analysis of this issue, including in a proper way the radiative corrections to the scalar potential, was carried out in ref. [24]. The most relevant results obtained there for our present task are the following.

There are two types of constraints: the ones arising from directions in the field-space along which the (tree-level) potential can become unbounded from below (UFB), and those arising from the existence of charge and color breaking (CCB) minima in

the potential deeper than the standard minimum. By far, the most restrictive bounds are the UFB ones, and therefore we will concentrate on them here.

There are three UFB directions, labelled as UFB-1, UFB-2, UFB-3 in [24]. It is worth mentioning here that in general the unboundedness is only true at tree-level since radiative corrections eventually raise the potential for large enough values of the fields, but still these minima can be deeper than the realistic one (i.e. the SUSY SM vacuum) and thus dangerous. The UFB-3 direction, which involves the scalar fields $\{H_u, \nu_{L_i}, e_{L_j}, e_{R_j}\}$ with $i \neq j$ and thus leads also to electric charge breaking, yields the strongest bound among all the UFB and CCB constraints. For future convenience, let us briefly give the explicit form of this constraint. By simple analytical minimization of the relevant terms of the scalar potential it is possible to write the value of all the $\nu_{L_i}, e_{L_j}, e_{R_j}$ fields in terms of the H_u one. Then, for any value of $|H_u| < M_{GUT}$ satisfying

$$|H_u| > \sqrt{\frac{\mu^2}{4\lambda_{e_j}^2} + \frac{4m_{L_i}^2}{g'^2 + g_2^2}} - \frac{|\mu|}{2\lambda_{e_j}} \ , \tag{2}$$

the value of the potential along the UFB-3 direction is simply given by

$$V_{\rm UFB-3} = (m_{H_u}^2 + m_{L_i}^2)|H_u|^2 + \frac{|\mu|}{\lambda_{e_j}}(m_{L_j}^2 + m_{e_j}^2 + m_{L_i}^2)|H_u| - \frac{2m_{L_i}^4}{g'^2 + g_2^2} \ . \tag{3}$$

Otherwise

$$V_{\rm UFB-3} = m_{H_u}^2|H_u|^2 + \frac{|\mu|}{\lambda_{e_j}}(m_{L_j}^2 + m_{e_j}^2)|H_u| + \frac{1}{8}(g'^2 + g_2^2)\left[|H_u|^2 + \frac{|\mu|}{\lambda_{e_j}}|H_u|\right]^2 \ . \tag{4}$$

In eqs. (3) and (4) λ_{e_j} is the leptonic Yukawa coupling of the $j-$generation. Then, the UFB-3 condition reads

$$V_{\rm UFB-3}(Q = \hat{Q}) > V_{\rm real\ min} \ , \tag{5}$$

where $V_{\rm real\ min} = -\frac{1}{8}(g'^2 + g_2^2)(v_u^2 - v_d^2)^2$, with $v_{u,d} = \langle H_{u,d}^0 \rangle$, is the realistic minimum evaluated at the typical scale of SUSY masses, say M_{SUSY} (normally, as mentioned in the Introduction, a good choice for M_{SUSY} is an average of the stop masses), and the renormalization scale $\hat{Q}$ is given by $\hat{Q} \sim {\rm Max}(\lambda_{top}|H_u|, M_{SUSY})$. Notice from eqs. (3) and (4) that the negative contribution to V_{UFB-3} is essentially given by the $m_{H_u}^2$ term, which can be very sizeable in many instances. On the other hand, the positive contribution is dominated by the term $\propto 1/\lambda_{e_j}$, thus the larger λ_{e_j} the more restrictive the constraint becomes. Consequently, the optimum choice of the $e-$type slepton is the third generation one, i.e. $e_j =$ stau.

3 Experimental and astrophysical constraints

As mentioned in the Introduction, we have to be sure that we obtain a correct phenomenology in our analysis. In this sense, we list here the most recent experimental

and astrophysical results which are relevant when computing the neutralino-nucleon cross section in the context of SUGRA. They give rise to important constraints on the parameter space.

- Higgs mass

  Whereas in the context of the SM the negative direct search for the Higgs at the LEP2 collider implies a precise lower bound on its mass of 114.1 GeV, the situation in SUSY scenarios is more involved. In particular, in the framework of mSUGRA, one obtains [32] for the lightest CP-even Higgs $m_h \gtrsim 114.1$ GeV when $\tan\beta \lesssim 50$, and $m_h \gtrsim 91$ GeV when $\tan\beta$ is larger. This is because the ZZh coupling, which controls the detection of the lightest MSSM Higgs at LEP, is $\sin^2(\alpha-\beta) \sim 1$ when $\tan\beta \lesssim 50$, and a significant suppression of $\sin^2(\alpha-\beta)$ occurs only with $\tan\beta > 50$. Recall in this sense that α is the Higgs mixing angle in the neutral CP-even Higgs sector, and $\sigma_{SUSY}(e^+e^- \to Zh) = \sin^2(\alpha-\beta)\sigma_{SM}(e^+e^- \to Zh)$ [33]. Let us remark anyway that generically $\tan\beta$ is constrained to be $\tan\beta \lesssim 60$, since otherwise several problems arise. For example, for moderate values of m and M, the squared CP-odd Higgs mass, m_A^2, becomes negative, unless a fine-tuning (in the sense that only certain combinations of m and M are possible) is carried out. In our computation below we will analyse values of $\tan\beta$ from 10 to 50.

  Clearly, from the above discussion, when the mSUGRA framework is relaxed $\sin^2(\alpha-\beta)$ must be computed for all points of the parameter space in order to know which bound for the lightest MSSM Higgs must be applied [34].

  Let us finally remark that we evaluate m_h using the program `FeynHiggsFast`, a simplified version of the updated program `FeynHiggs` [35] which contains the complete one-loop and dominant two-loop corrections. The value of m_h obtained with `FeynHiggsFast` is approximately 1 GeV below the one obtained using `FeynHiggs`. In addition, although the value of m_h obtained with FeynHiggs has an uncertainty of about 3 GeV, due e.g. to higher-order corrections, we have no taken it into account in our computation.

- Top mass

  Needless to say we use as input for the top mass throughout this paper the central experimental value $m_t(pole) = 175$ GeV. However, let us remark that a modification in this mass by ± 1 GeV implies, basically, a modification also of ± 1 GeV in the value of m_h obtained here.

- Bottom and tau masses

  For the bottom mass we take as input $m_b(m_b) = 4.25$ GeV, which, following the analysis of ref. [36] with $\alpha_s(M_Z) = 0.1185$, corresponds to $m_b(M_Z) = 2.888$ GeV. In the evolution of the bottom mass we incorporate the SUSY threshold corrections [37] at M_{SUSY}. These are known to be significant, specially for large values of $\tan\beta$. We also follow a similar analysis for the tau mass, using as input $m_\tau(M_Z) = 1.7463$ GeV.

- SUSY spectrum

  We impose the present experimental lower bounds on SUSY masses coming from LEP and Tevatron. In particular, using the low-energy relation from mSUGRA, $M_1 = \frac{5}{3}\tan^2\theta_W M_2$, one obtains for the lightest chargino mass the bound [38] $m_{\tilde{\chi}_1^\pm} > 103$ GeV. Likewise, one is also able to obtain the following bounds for sleptons masses [39]: $m_{\tilde{e}} > 99$ GeV, $m_{\tilde{\mu}} > 96$ GeV, $m_{\tilde{\tau}} > 87$ GeV. Finally, we use the following bounds on the masses of the sneutrino, the lightest stop, the rest of squarks, and gluinos: $m_{\tilde{\nu}} > 50$ GeV, $m_{\tilde{t}} > 95$ GeV, $m_{\tilde{q}} > 150$ GeV, $m_{\tilde{g}} > 190$ GeV.

- $b \to s\gamma$

  The measurements of $B \to X_s\gamma$ decays at CLEO [40] and BELLE [41], lead to bounds on the branching ratio $b \to s\gamma$. In particular we impose on our computation $2\times10^{-4} \leq BR(b \to s\gamma) \leq 4.1\times10^{-4}$, where the evaluation is carried out using the routine provided by the program `micrOMEGAs` [42]. A description of this procedure can be found in ref. [43]. Although the improvements of ref. [44] are not included in this routine, they are not so important for our study since we consider only $\mu > 0$.

- $g_\mu - 2$

  The new measurement of the anomalous magnetic moment of the muon, $a_\mu = (g_\mu - 2)/2$, in the E821 experiment at the BNL [45] deviates by $(33.7 \pm 11.2)\times10^{-10}$ from the recent SM calculation of ref. [46] using e^+e^- data. Assuming that the possible new physics is due to SUGRA, we will show in our computation the constraint $11.3 \times 10^{-10} \leq a_\mu(SUGRA) \leq 56.1 \times 10^{-10}$ at the 2σ level. This would exclude the case $\mu < 0$. However, it is worth noticing that the above result is in contradiction with the one obtained by using tau decay data (instead of e^+e^- ones) which only imply a deviation $(9.4 \pm 10.5) \times 10^{-10}$ from the SM calculation [46].

- LSP

  The lightest supersymmetric particle (LSP) must be an electrically neutral (also with no strong interactions) particle, since otherwise it would bind to nuclei and would be excluded as a candidate for dark matter from unsuccessful searches for exotic heavy isotopes [47]. Although the $\tilde{\chi}_1^0$ is the LSP in most of the parameter space of SUGRA, in some regions one of the staus, $\tilde{\tau}_1$, can be lighter. Therefore, following the above argument, we discard these regions.

- Relic $\tilde{\chi}_1^0$ density

  We impose in general the preferred astrophysical bounds on the dark matter density, $0.1 \lesssim \Omega_{DM}h^2 \lesssim 0.3$, on our theoretical computation of the relic $\tilde{\chi}_1^0$ density, assuming $\Omega_{DM} \approx \Omega_{\tilde{\chi}_1^0}$. For the sake of completeness we also show in the figures the bounds $0.094 \lesssim \Omega_{DM}h^2 \lesssim 0.129$ deduced from the recent data obtained by

the WMAP satellite [48]. Let us remark that the theoretical computation of the relic density depends on assumptions about the evolution of the early Universe, and therefore different cosmological scenarios give rise to different results [49]. We will consider in our analysis the standard mechanism of thermal production of neutralinos.

Let us finally mention that we evaluate $\Omega_{\tilde{\chi}_1^0}$ using the program `microMEGAs` [42]. The exact tree-level cross sections for all possible annihilation [50] and coannihilation [51, 52, 53] channels are included in the code through a link to `CompHEP` [54], and accurate thermal average of them is used. Also, poles and thresholds are properly handled and one-loop QCD corrected Higgs decay widths [55] are used. The SUSY corrections included in the latest version of the code [55] are not implemented yet by `micrOMEGAs`. Fortunately, in our case, their effect is much smaller than that of the QCD corrections. Good agreement between `micrOMEGAs` and other independent computations of $\Omega_{\tilde{\chi}_1^0}$ including $\tilde{\chi}_1^0 - \tilde{\tau}_1$ coannihilations can be found in ref. [56].

4 mSUGRA predictions for the neutralino-nucleon cross section

Let us recall first that the relevant effective Lagrangian describing the elastic scattering of $\tilde{\chi}_1^0$ on protons and neutrons has a spin-independent (scalar) interaction and a spin-dependent interaction [50]. However, the contribution of the scalar one is generically larger and therefore we will concentrate on it. This scalar interaction includes contributions from squark exchange and neutral Higgs exchange. Let us also remark that the scalar cross sections for both, protons and neutrons, are basically equal. Taking all the above into account, in this section we will compute the predictions for the scalar neutralino-proton cross section $\sigma_{\tilde{\chi}_1^0-p}$ in the context of mSUGRA, where the soft terms are assumed to be universal. As discussed in the Introduction, this is the simplest possibility and may arise in specific string constructions. In particular we will carry out the analysis following first the usual assumption of a GUT scale, $M_{GUT} \approx 2\times 10^{16}$ GeV, and later we will modify this assumption allowing the possibility of an intermediate scale.

4.1 GUT scale

As is well known, in the mSUGRA scenario with a GUT scale $\tilde{\chi}_1^0$ is mainly bino and, as a consequence, the predicted $\sigma_{\tilde{\chi}_1^0-p}$ is well below the accessible experimental regions for low and moderate values of $\tan\beta$. We show this fact in Fig. 1, where contours of $\sigma_{\tilde{\chi}_1^0-p}$ in the parameter space (m, M) for $\tan\beta = 10$ and $\mu > 0$ are plotted for different values of A. We choose A proportional to M because this relation is particularly interesting, arising naturally in several string models [10]. However our conclusions will be independent on this assumption. For example, if we choose to do the plots for different constant values of A, a very common procedure in pure SUGRA

analyses, the results will be qualitatively similar. Let us also remark that the sign of the dominant contribution to the supersymmetric contribution to the muon anomalous magnetic moment is given by $M_2\mu$. As we discussed in the previous section, we are taking this to be positive, and therefore we will only consider $sign(M) = sign(\mu)$. Now, due to the symmetry of the RGEs, the results for $(-M, A, -\mu)$ are identical to those for $(M, -A, \mu)$, and therefore, we can cover the whole (permitted) parameter space restricting to positive values for M and μ and allowing A to take positive and negative values. On the other hand, note that we can deduce the value of the $\tilde{\chi}_1^0$ mass in the plots from the value of M, since $m_{\tilde{\chi}_1^0} \sim 0.4\ M$. For the gluino mass we can also use the simple relation, $m_{\tilde{g}} \sim 2.5\ M$.

As we can see in the figure, the experimental bounds discussed in Section 3 are very important and exclude large regions of the parameter space. For example, for $A = 2M$ the whole parameter space is forbidden. This is due to the combination of the Higgs mass bound with the $g_\mu - 2$ lower bound (recall that we are using only the limit based on e^+e^- analysis). Notice in this sense that the bound on the Higgs mass is less restrictive for smaller values of A, and therefore the allowed region is relatively large for $A = 0, -M$. For example, for $A = 0$ one obtains from the Higgs mass the lower bound $M \gtrsim$ 320 GeV, and from $g_\mu - 2$ the upper bound $M \lesssim$ 440 GeV. These bounds imply for the neutralino, $128 \lesssim m_{\tilde{\chi}_1^0} \lesssim 176$ GeV, and for the gluino (and squarks) $800 \lesssim m_{\tilde{g}} \lesssim 1100$ GeV. The light shaded area in Fig. 1 shows the region allowed by the experimental bounds. There, the lower contour is obtained including also the constraint coming from the LSP bound. On the other hand, when the astrophysical bounds $0.1 \lesssim \Omega_{\tilde{\chi}_1^0} h^2 \lesssim 0.3$ are also imposed the allowed area becomes very small (extremely small if the recent WMAP data are taken into account). Only the beginning of the tail where the LSP is almost degenerate with the stau, producing efficient coannihilations, is rescued. For $A = -M$ a small part of the bulk region with moderate m and M is also rescued. For this area $\sigma_{\tilde{\chi}_1^0 - p} \approx 10^{-9}$ pb.

In addition, the restrictions coming from the UFB-3 constraint discussed in Section 2 exclude also this area. We have checked that this is also true for smaller values of A, as e.g. $A = -2M$. Let us remark that this constraint depends crucially on the value of A. In particular the UFB-3 excluded (ruled) region is larger for negative values of A and also increases with $|A|$ as shown in Fig. 1. This can be understood from the evolution of $m_{H_u}^2$ with the scale, since for the above cases it becomes more negative. From the discussion concerning eqs. (3) and (4) we deduce that the negative contribution to V_{UFB-3} is more important and therefore the UFB-3 minima are easily deeper than the realistic one. Note that the region excluded because the stau is the LSP is also generically excluded by the UFB-3 constraint. Again, this can be understood from eqs. (3) and (4), since the positive contribution to V_{UFB-3} depends on the stau mass, and this is now small. In conclusion, the results indicate that the whole parameter space for $\tan\beta = 10$ is excluded on these grounds. It is worth noticing, however, that when the $g_\mu - 2$ lower bound is relaxed, for large values of M a narrow region of the area fulfilling the astrophysical bounds might be allowed for the case $A = M$.

Although the cross section increases, entering in the DAMA region [2, 3], when the value of $\tan\beta$ increases [57, 58], the present experimental constraints exclude this

possibility [11, 59]. We show this fact in Fig. 2 for $\tan\beta = 35$ and four representative values of A. In principle, if we only impose the LEP lower bound $m_{\tilde{\chi}_1^\pm} > 103$ GeV, the cross section can be as large as $\sigma_{\tilde{\chi}_1^0-p} \approx 10^{-6}$ pb. However, at the end of the day, the other experimental bounds (Higgs mass, $b \to s\gamma$, $g_\mu - 2$ upper bound) constrain the cross section to be $\sigma_{\tilde{\chi}_1^0-p} \lesssim 10^{-8}$ pb. The region allowed by the $g_\mu - 2$ lower bound is now larger and the cross section can be as low as $\sigma_{\tilde{\chi}_1^0-p} \gtrsim 10^{-10}$ pb. For example, for $A = 0$ (and similarly for the others) these bounds imply $260 \lesssim M \lesssim 750$ GeV, and therefore $104 \lesssim m_{\tilde{\chi}_1^0} \lesssim 300$ GeV, $650 \lesssim m_{\tilde{g},\tilde{q}} \lesssim 1875$ GeV.

Concerning the UFB-3 constraint, it is worth noticing, by comparison with Fig. 1, that the larger $\tan\beta$ is, the larger the excluded region becomes. This is because the positive contribution for V_{UFB-3} is multiplied by the inverse of the tau Yukawa coupling. Since this coupling is proportional to $\frac{1}{\cos\beta}$, it increases when $\tan\beta$ increases leading to a decrease in the positive contribution. As a consequence the UFB-3 constraint becomes more restrictive. However, unlike the case $\tan\beta = 10$, this is not sufficient to forbid the whole dark shaded area allowed also by the astrophysical bounds, because the increase in the tau coupling also produces an increase of the region where the stau is the LSP, and therefore the coannihilation tail is also risen. This is very clear for $A = M$, where the region forbidden by the LSP bound is even larger than the one forbidden by the UFB-3. Since the area bounded by solid lines, fulfilling $0.1 \leq \Omega_{\tilde{\chi}_1^0} h^2 \leq 0.3$, has the lower edge above and very close to the LSP line (recall that coannihilations are very important in this region producing the correct amount of relic neutralino density), we can always find values of the parameters where all constraints are fulfilled. In fact, one can check that $\tan\beta > 20$ is needed to obtain this result. In any case, it is worth noticing that, even for these large values of $\tan\beta$, the UFB-3 constraint can be very important depending on the value of A. For example, in Fig. 2 a large region of the dark shaded area turns out to be forbidden when $A = 0$, and the whole region when $A = -M, -2M$.

The above comments can also be applied for very large values of $\tan\beta$, as e.g. $\tan\beta = 50$. We show this in Fig. 3. Note that now for $A = 0, -M, -2M$, unlike the case $\tan\beta = 35$, the whole dark shaded areas allowed by experimental and astrophysical bounds are not constrained by the UFB-3. Let us finally recall that the region allowed by $0.1 \leq \Omega_{\tilde{\chi}_1^0} h^2 \leq 0.3$ is larger because the CP-odd Higgs A becomes lighter as $\tan\beta$ increases. This allows the presence of resonances in the Higgs mediated annihilation channels, resulting in drastic reduction of the neutralino relic abundance. In the case of $\tan\beta = 50$, the resonant effects in the annihilation channels are felt in the whole parameter space displayed in Fig. 2. We can see as well, that for $A = M, 0$ the area of the parameter space where $\tilde{\chi}_1^0 - \tilde{\tau}_1$ coannihilations are relevant lead to values of $\Omega_{\tilde{\chi}_1^0} h^2 < 0.1$.

In Figs. 4 and 5 we summarize the above results for $\tan\beta = 35, 50$, concerning the cross section, showing the values of $\sigma_{\tilde{\chi}_1^0-p}$ allowed by all experimental constraints as a function of the neutralino mass $m_{\tilde{\chi}_1^0}$, for different values of A. Note that the gaugino mass M is essentially fixed for a given $\tan\beta$ and $m_{\tilde{\chi}_1^0}$. Dark grey dots correspond to those points having a relic neutralino density within the preferred range $0.1 \leq \Omega h^2 \leq 0.3$. Given the narrow range of these points for the case $\tan\beta = 35$, they overlap in

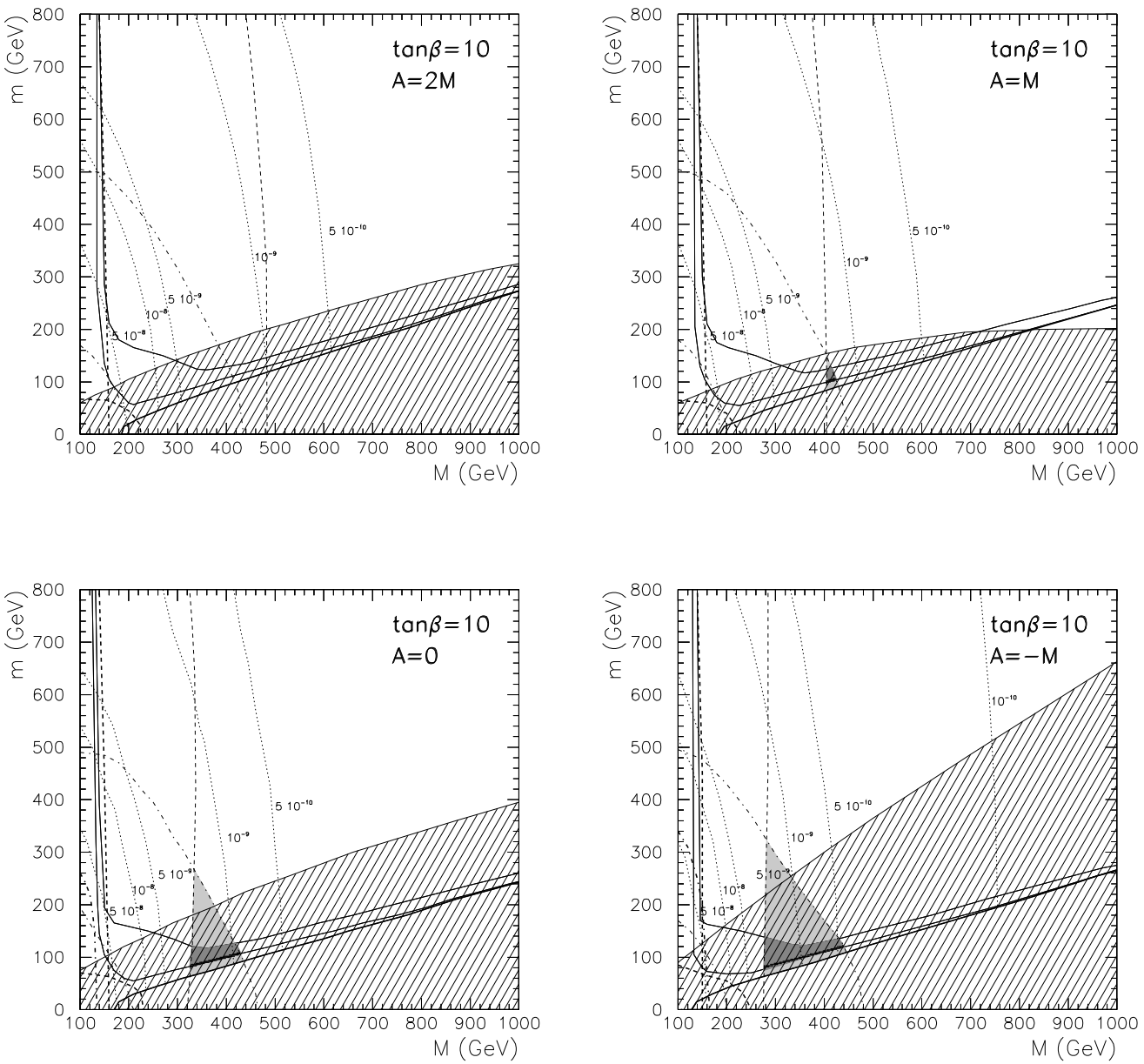

Figure 1: Scalar neutralino-proton cross section $\sigma_{\tilde{\chi}_1^0-p}$ in the parameter space of the mSUGRA scenario (m, M) for $\tan\beta = 10$ and $\mu > 0$, using different values of A. The dotted curves are contours of $\sigma_{\tilde{\chi}_1^0-p}$. The region to the left of the near-vertical dashed line is excluded by the lower bound on the Higgs mass $m_h > 114.1$ GeV. The region to the left of the near-vertical double dashed line is excluded by the lower bound on the chargino mass $m_{\tilde{\chi}_1^\pm} > 103$ GeV. The corner in the lower left shown also by a double dashed line is excluded by the LEP bound on the stau mass $m_{\tilde{\tau}_1} > 87$ GeV. The region bounded by dot-dashed lines is allowed by $g_\mu - 2$. The region to the left of the double dot-dashed line is excluded by $b \to s\gamma$. From bottom to top, the solid lines are the upper bounds of the areas such as $m_{\tilde{\tau}_1} < m_{\tilde{\chi}_1^0}$ (double solid), $\Omega_{\tilde{\chi}_1^0}h^2 < 0.1$ and $\Omega_{\tilde{\chi}_1^0}h^2 < 0.3$. The light shaded area is favored by all the phenomenological constraints, while the dark one fulfils in addition $0.1 \leq \Omega_{\tilde{\chi}_1^0}h^2 \leq 0.3$ (the black region on top of this indicates the WMAP range $0.094 < \Omega_{\tilde{\chi}_1^0}h^2 < 0.129$). The ruled region is excluded because of the charge and colour breaking constraint UFB-3.

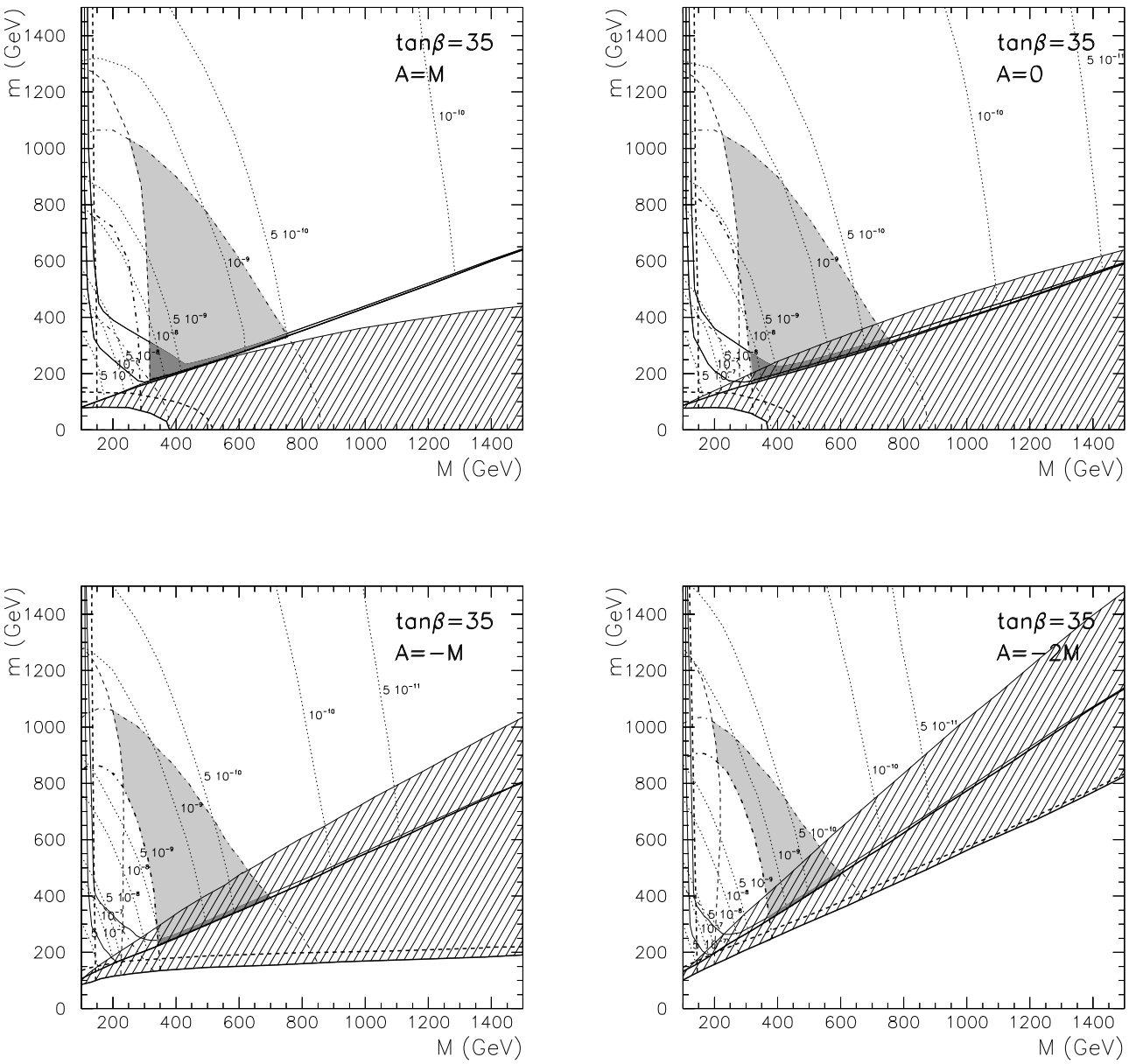

Figure 2: The same as in Fig. 1 but for $\tan\beta = 35$ and different values of A. The white region at the bottom bounded by a solid line is excluded because $m^2_{\tilde{\tau}_1}$ becomes negative.

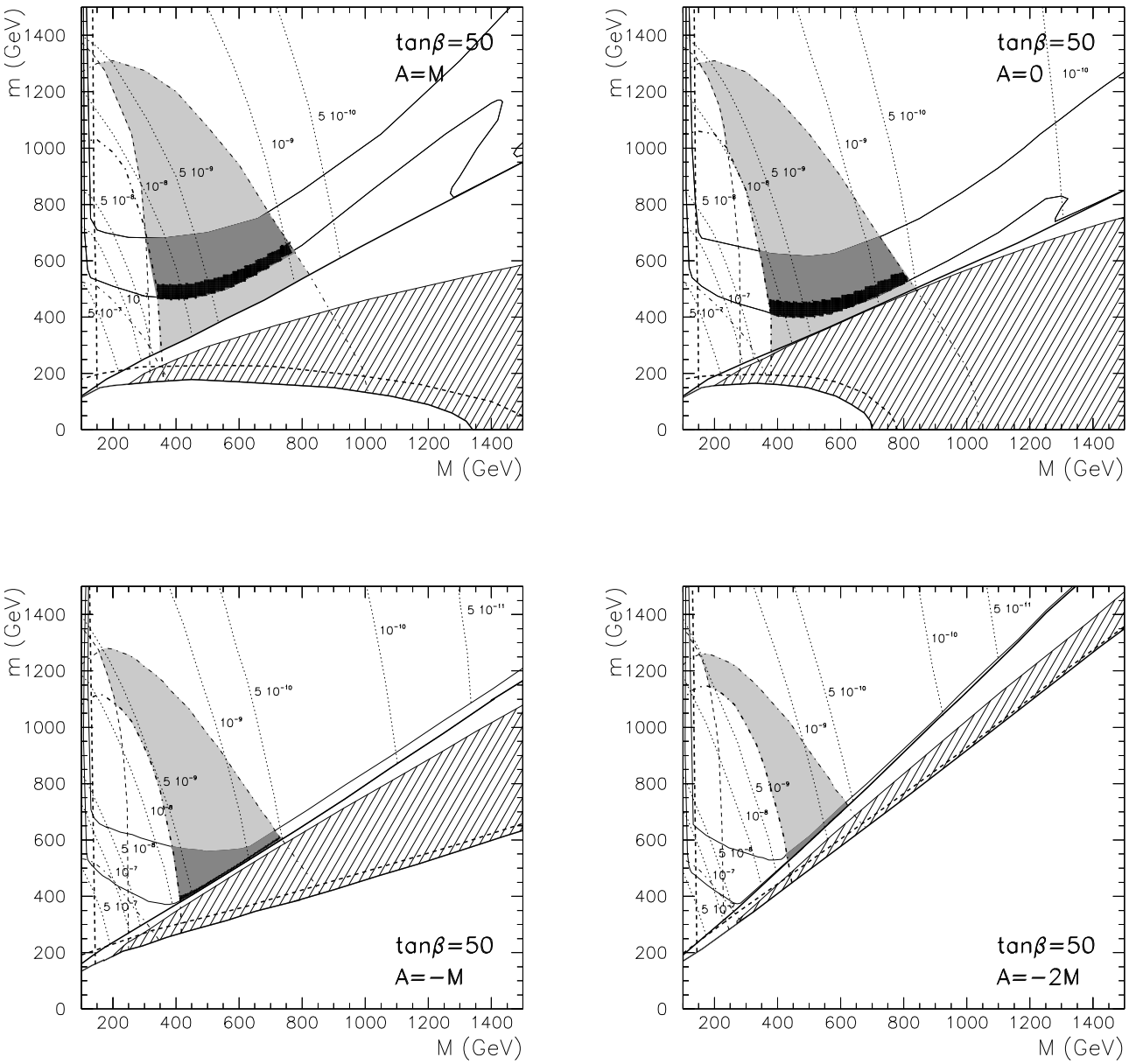

Figure 3: The same as in Fig. 1 but for $\tan\beta = 50$ and different values of $A = M$. The white region at the bottom bounded by a solid line is excluded because $m^2_{\tilde{\tau}_1}$ becomes negative.

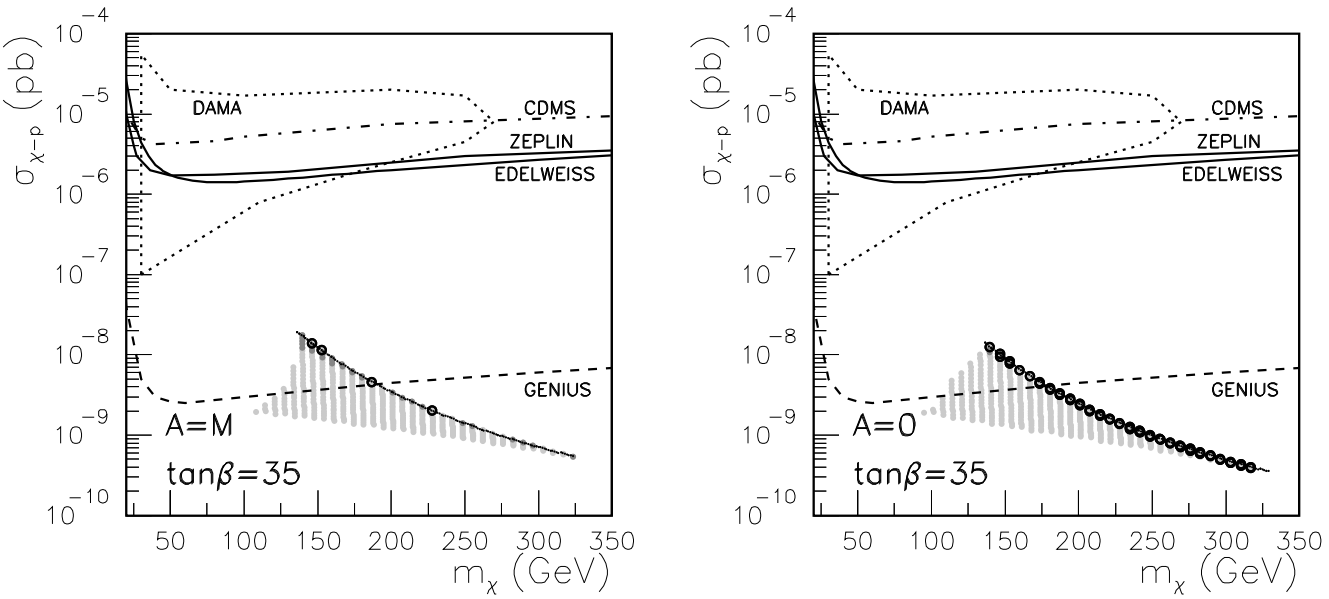

Figure 4: Scatter plot of the scalar neutralino-proton cross section $\sigma_{\tilde{\chi}_1^0-p}$ as a function of the neutralino mass $m_{\tilde{\chi}_1^0}$ in the mSUGRA scenario, for $\tan\beta = 35$ and $A = M, 0$, with $\mu > 0$. The light grey dots correspond to points fulfilling all experimental constraints. The dark grey dots correspond to points fulfilling in addition $0.1 \leq \Omega_{\tilde{\chi}_1^0} h^2 \leq 0.3$ (the black dots on top of these indicate those fulfilling the WMAP range $0.094 < \Omega_{\tilde{\chi}_1^0} h^2 < 0.129$). The circles indicate regions excluded by the UFB-3 constraint. The area bounded by dotted lines is allowed by the DAMA experiment [2, 3]. The (upper) areas bounded by dot-dashed and solid lines are excluded by CDMS [4] and EDELWEISS [5] and ZEPLIN I [7] current experimental limits. The (upper) area bounded by the dashed line will be analized by the projected GENIUS experiment [60].

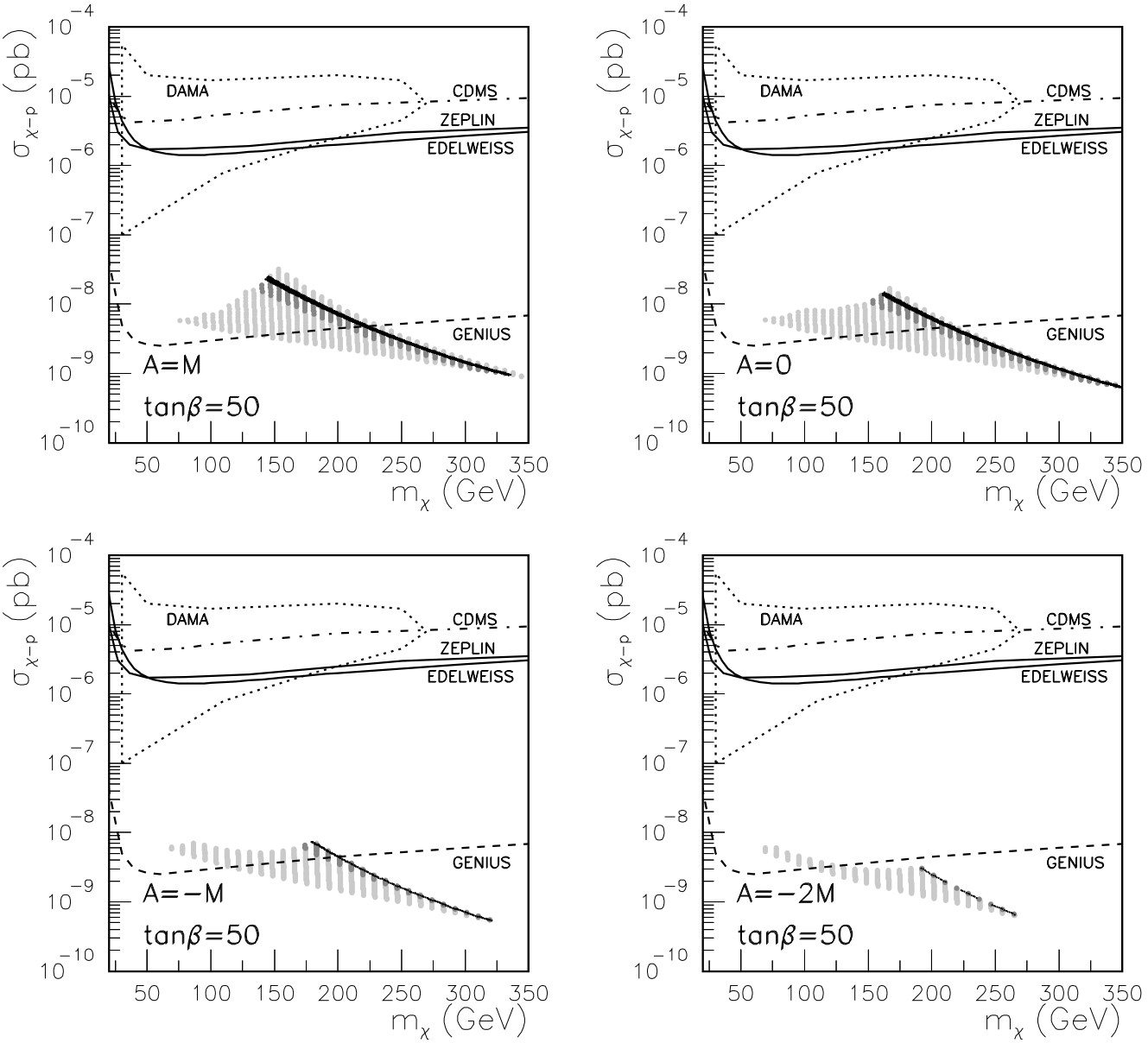

Figure 5: The same as in Fig. 4 but for $\tan\beta = 50$ and different values of A.

the figure for $A = 0$ with those excluded by the UFB-3 constraint (shown with circles). We observe that, generically, the cross section and the neutralino mass are constrained to be $5 \times 10^{-10} \lesssim \sigma_{\tilde{\chi}_1^0-p} \lesssim 3 \times 10^{-8}$ pb and $120 \lesssim m_{\tilde{\chi}_1^0} \lesssim 320$ GeV, respectively.

Obviously, in this mSUGRA case, more sensitive detectors producing further data are needed[1]. Fortunately, many dark matter detectors are being projected. Particularly interesting is the case of GENIUS [60], where values of the cross section as low as $\approx 10^{-9}$ pb will be accessible, as shown in Figs. 4 and 5. It is worth noticing here that the DAMA area shown in the Figures, has been obtained in ref. [3] taking into account the effect of the galactic halo modeling on the DAMA annual modulation result. This area is larger than in the case of considering just the standard (isothermal sphere) model. On the other hand, for the other experiments similar analyses taking into account the uncertainties in the galactic halo are not available, and we use in the Figures the effect of the standard halo model on their results. Including these uncertainties, the region favoured by DAMA and not excluded by the null searches would be in principle smaller than the one shown here.

4.2 Intermediate scale

The analysis of the cross section $\sigma_{\tilde{\chi}_1^0-p}$ carried out above in the context of mSUGRA, was performed assuming the unification scale $M_{GUT} \approx 10^{16}$ GeV. However, there are several interesting phenomenological arguments in favour of SUGRA scenarios with scales $M_I \approx 10^{10-14}$ GeV (for a review see e.g. ref. [62]). In addition, the string scale may be anywhere between the weak and the Planck scale, and explicit scenarios with intermediate scales may arise in the context of D-brane constructions from type I strings [63]. In this sense, to use the value of the initial scale, say M_I, as a free parameter for the running of the soft terms is particularly interesting. In fact, it was pointed out in refs. [64, 65, 63] that $\sigma_{\tilde{\chi}_1^0-p}$ is very sensitive to the variation of the initial scale for the running of the soft terms. For instance, by taking $M_I = 10^{10-12}$ GeV rather than M_{GUT}, and non-universal gauge couplings, regions in the parameter space of mSUGRA can be found where $\sigma_{\tilde{\chi}_1^0-p}$ is two orders of magnitude larger than for M_{GUT} [64, 15].

The fact that smaller scales imply a larger $\sigma_{\tilde{\chi}_1^0-p}$ can be explained with the variation in the value of μ with M_I. One observes that, for $\tan\beta$ fixed, the smaller the initial scale for the running the smaller the numerator in the first piece of eq. (1) becomes. This can be understood from the well known evolution of $m_{H_u}^2$ with the scale. Clearly, when the value of the initial scale is reduced the RGE running is shorter and, as a consequence, the negative contribution $m_{H_u}^2$ to μ^2 in eq. (1) becomes less important. Then, $|\mu|$ decreases and therefore the Higgsino composition of the lightest neutralino increases. Eventually, $|\mu|$ will be of the order of M_1, M_2 and $\tilde{\chi}_1^0$ will be a mixed Higgsino-gaugino state. In addition, when $|\mu|$ decreases the (tree-level) mass of the CP-odd Higgs, $m_A^2 = m_{H_d}^2 + m_{H_u}^2 + 2\mu^2$ decreases. Since the heaviest CP-even Higgs, H, is almost degenerate in mass with this, it also decreases significantly. Indeed, scattering channels

[1] For a different conclusion, using a phenomenological SUSY model whose parameters are defined directly at the electroweak scale, see ref. [61].

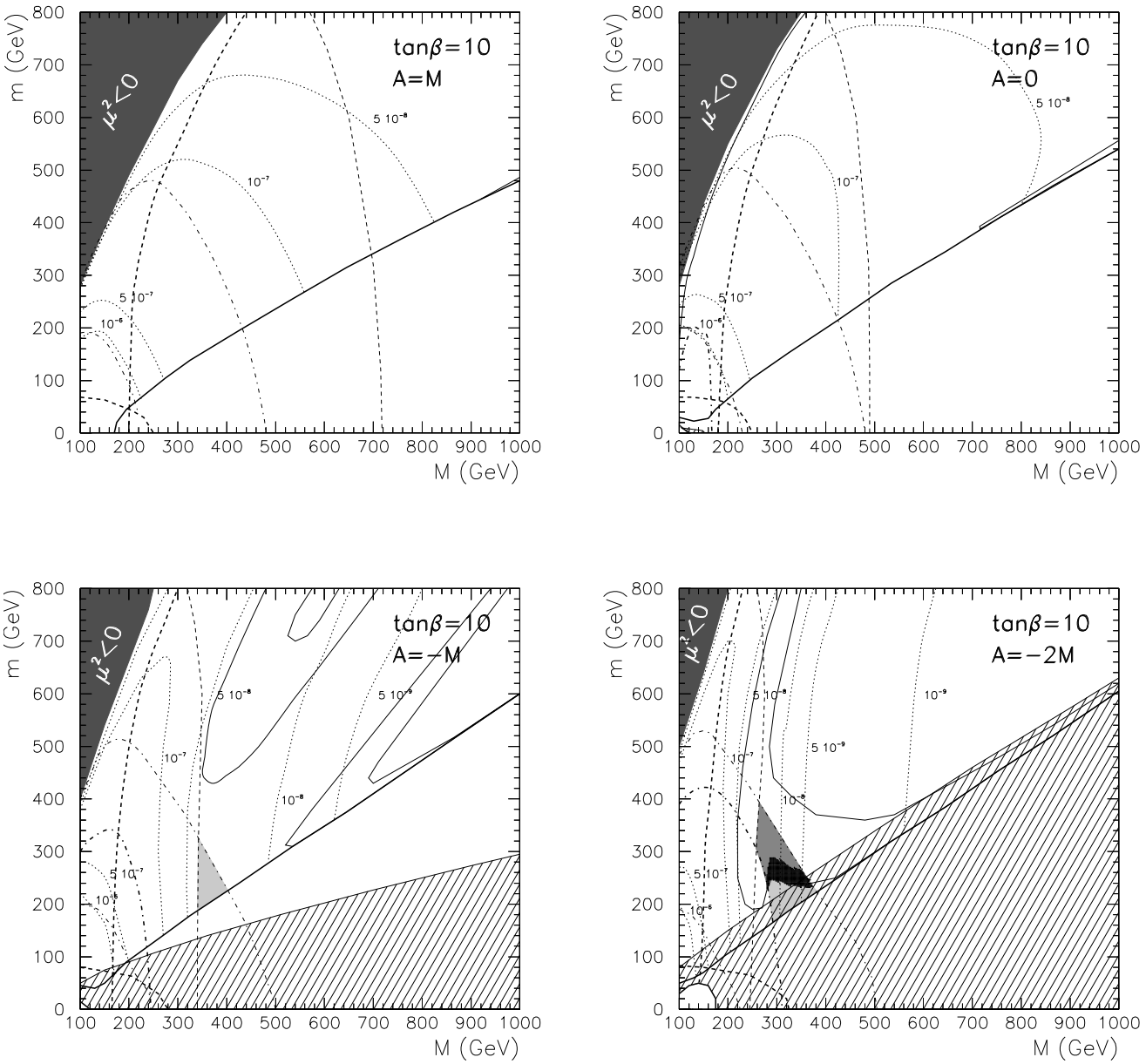

Figure 6: The same as in Fig. 1 but for the intermediate scale $M_I = 10^{11}$ GeV, with $\tan\beta = 10$ and different values of A. The black area is excluded because μ^2 becomes negative. The white region at the bottom bounded by a solid line is excluded because $m^2_{\tilde{\tau}_1}$ becomes negative.

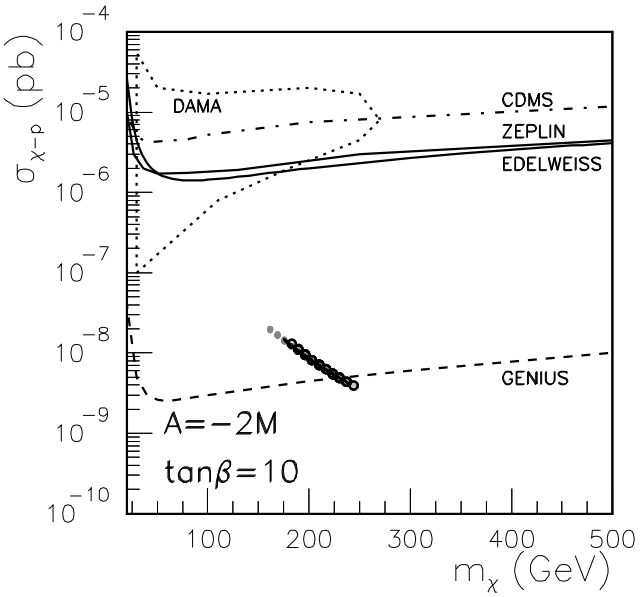

Figure 7: The same as in Fig. 4 but for the intermediate scale $M_I = 10^{11}$ GeV, with $\tan\beta = 10$ and $A = -2M$.

through Higgs exchange are very important and their contributions to the cross section will increase it. Let us also remark that, for the same value of the parameters, the Higgs mass m_h decreases with respect to the GUT scale scenario. This is because the value of m_h depends on the value of the gluino mass M_3. It increases when M_3 increases at low energy. However, now the running is shorter and therefore M_3 at low energy is smaller than in the GUT scenario. Although the latter may be welcome in order to obtain larger cross sections, it may also be dangerous when confronting with the experimental result concerning the Higgs mass.

Concerning the value of the relic density, $\Omega_{\tilde{\chi}_1^0}$ is dramatically reduced with respect to the M_{GUT} case. This is due to a combination of several factors: 1) The Higgsino-gaugino composition of $\tilde{\chi}_1^0$ allows a significant increase of the $\tilde{\chi}_1^0$ annihilation cross section, due to channels with Higgs and gauge bosons in the final states; 2) The decrease of the mass of the pseudoscalar Higgs, along with the value of the μ–term, enables the presence of resonant annihilation channels even at $\tan\beta = 10$; 3) The masses of the lightest chargino and stop are small enough to allow $\tilde{\chi}_1^0$–$\tilde{\chi}_1^\pm$ [52] and $\tilde{\chi}_1^0$–$\tilde{t}_1$ [53] coannihilations in some areas of the parameter space. Although the later is less relevant, we find some areas at $\tan\beta = 50$ and $A < 0$.

We show in Fig. 6 the result for $M_I = 10^{11}$ GeV, with $\tan\beta = 10$. This can be compared with the one in Fig. 1, where M_{GUT} is used. Now the relation $m_{\tilde{\chi}_1^0} \sim 0.4\ M$ does not hold, and one has $m_{\tilde{\chi}_1^0} > 0.4M$. In any case, $m_{\tilde{\chi}_1^0} < M_1$ since the bino-Higgsino mixing is significant in this case. Clearly, for the same values of the parameters, larger cross sections can be obtained with the intermediate scale. It is worth noticing that even with this moderate value of $\tan\beta$, $\tan\beta = 10$, there are regions where the cross

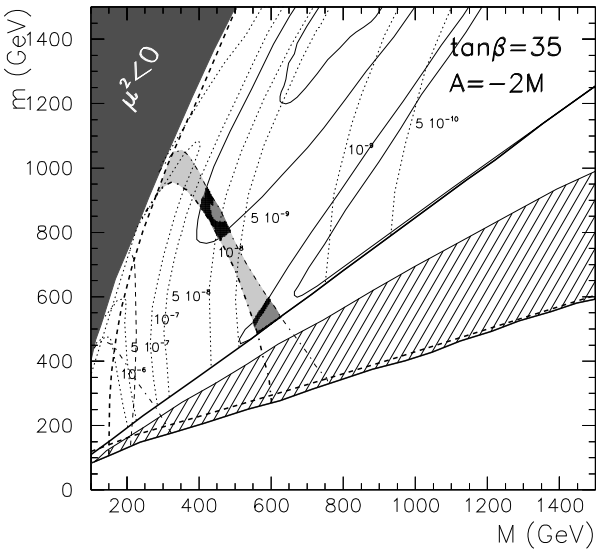

Figure 8: The same as in Fig. 6 but for $\tan\beta = 35$ and $A = -2M$.

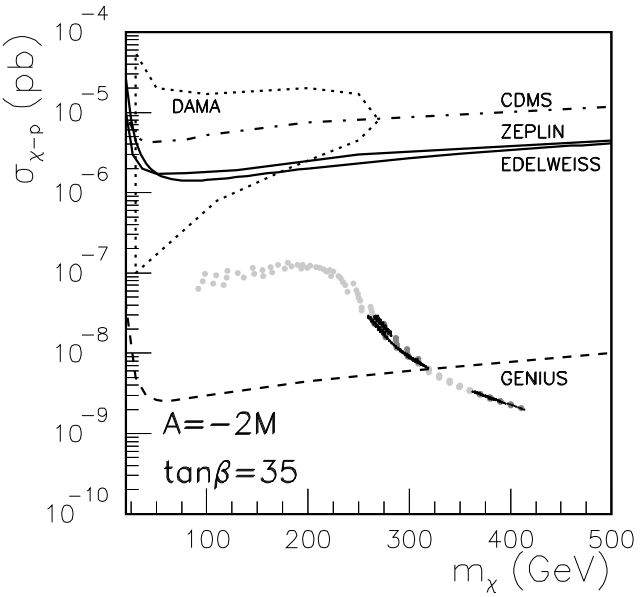

Figure 9: The same as in Fig. 7 but for $\tan\beta = 35$ and $A = -2M$.

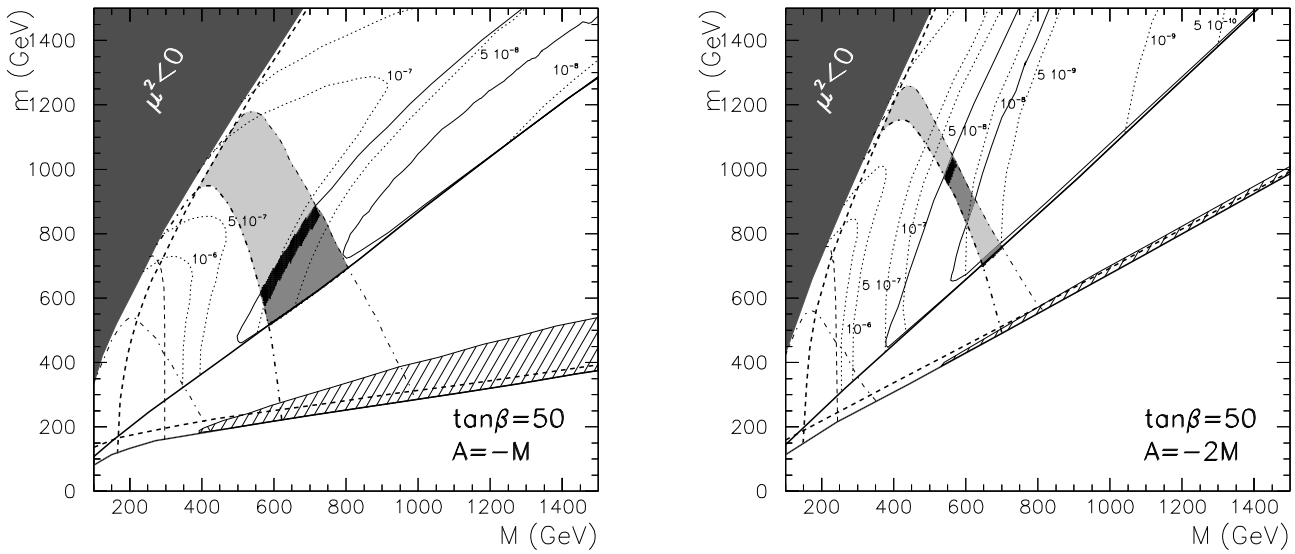

Figure 10: The same as in Fig. 6 but for $\tan\beta = 50$ and $A = -M, -2M$.

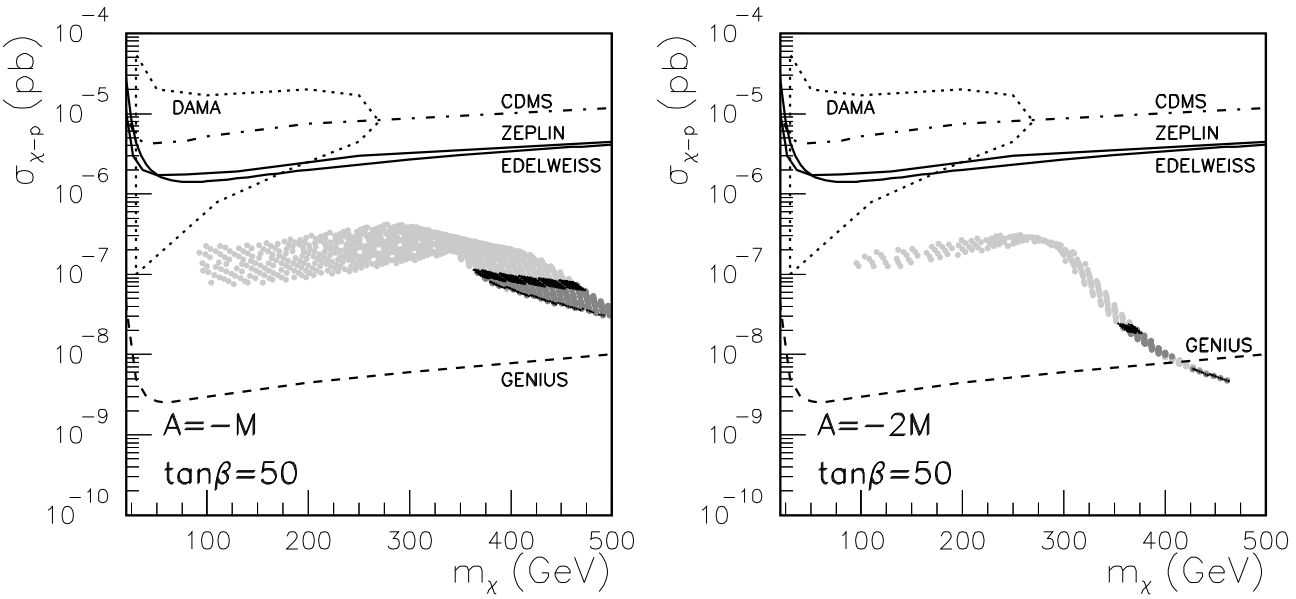

Figure 11: The same as in Fig. 7 but for $\tan\beta = 50$ and $A = -M, -2M$.

section enters in the DAMA area, $\sigma_{\tilde{\chi}_1^0-p} \approx 10^{-6}$ pb. However, for $A = M, 0$ the whole parameter space is forbidden due to the combination of the Higgs mass bound with the $g_\mu - 2$ lower bound. We have checked explicitly that 114.1 GeV is the correct lower bound to be used concerning the Higgs mass, since generically $\sin^2(\alpha - \beta) \sim 1$ for the intermediate scale. Notice also that now, for these values of A, $\Omega_{\tilde{\chi}_1^0} h^2$ is smaller than 0.1 in most of the parameter space. Only very small regions bounded by solid lines, and therefore with $0.1 \leq \Omega_{\tilde{\chi}_1^0} h^2 \leq 0.3$, can be found in both figures with $A = M, 0$. For $A = -M, -2M$ there are small regions where the m_h and $g_\mu - 2$ bounds are compatible, but finally the constraint $m_h > 114.1$ GeV implies that the allowed cross sections do not enter in the DAMA area. Although now larger regions with $0.1 \leq \Omega_{\tilde{\chi}_1^0} h^2 \leq 0.3$ are present, for $A = -M$ these are not compatible with the experimental bounds.

We also find that the region excluded by the UFB-3 constraint is much smaller than in those cases where the initial scale is the GUT one (see Fig. 1). In fact, only for $A = -2M$ this region is larger than the one forbidden by the LSP bound. As explained above, when the initial scale is smaller the negative value of $m_{H_u}^2$ becomes less important. Therefore the negative contribution to V_{UFB-3} is also less important. As a consequence, the UFB-3 minima are not so easily deeper than the realistic one [26] [2].

In Fig. 7 we summarize the above results for $\tan\beta = 10$, concerning the cross section, showing the values of $\sigma_{\tilde{\chi}_1^0-p}$ allowed by all experimental constraints as a function of the neutralino mass $m_{\tilde{\chi}_1^0}$, for $A = -2M$. Only in this case there are dark grey dots corresponding to points having a relic neutralino density within the preferred range $0.1 \leq \Omega_{\tilde{\chi}_1^0} h^2 \leq 0.3$. Given the narrow range of these points, they overlap in the figure with those excluded by the UFB-3 constraint. They correspond to $150 \lesssim m_{\tilde{\chi}_1^0} \lesssim 250$ GeV, and e.g. the mass of the lightest stop, $\tilde{t}_1$, is between 250 and 340 GeV.

Qualitatively, similar results are obtained for larger values of $\tan\beta$. For example, for $\tan\beta = 35$ and $A = M$ there are now regions in the parameter space with $\sigma_{\tilde{\chi}_1^0-p} \lesssim 3 \times 10^{-7}$ pb fulfilling all experimental constraints, however they have $\Omega_{\tilde{\chi}_1^0} h^2 < 0.03$. A similar situation occurs for $A = 0$, where $\Omega_{\tilde{\chi}_1^0} h^2 < 0.06$. On the other hand, for $A = -2M$ we obtain points allowed by all experimental and astrophysical constraints, and this is shown in Figs. 8 and 9. The upper bound in the cross section is because of the $b \to s\gamma$ process. Points within the preferred astrophysical range correspond to $\sigma_{\tilde{\chi}_1^0-p} \lesssim 10^{-8}$ pb. Now, there are two allowed regions with $275 \lesssim m_{\tilde{\chi}_1^0} \lesssim 325$ GeV and $370 \lesssim m_{\tilde{\chi}_1^0} \lesssim 420$ GeV. For these, $570 \lesssim m_{\tilde{t}_1} \lesssim 720$ GeV.

The situation for $\tan\beta = 50$ is shown in Figs. 10 and 11. Now, unlike the previous case, for $A = -M$ there are also points allowed by all experimental and astrophysical constraints, and $\sigma_{\tilde{\chi}_1^0-p} \lesssim 10^{-7}$ pb. In this case, for example for $A = -2M$, there are two allowed regions with $360 \lesssim m_{\tilde{\chi}_1^0} \lesssim 410$ GeV, $600 \lesssim m_{\tilde{t}_1} \lesssim 800$ GeV and $425 \lesssim m_{\tilde{\chi}_1^0} \lesssim 460$ GeV, $445 \lesssim m_{\tilde{t}_1} \lesssim 475$ GeV. We should mention that in the later the effect of $\tilde{\chi}_1^0$–$\tilde{t}_1$ is present in the estimation of $\Omega_{\tilde{\chi}_1^0} h^2$, however it is less significant than the $\tilde{\chi}_1^0$–$\tilde{\tau}_1$ one.

[2] This argument was used in ref. [29] to allow again the dilaton dominated supersymmetry breaking scenario, which was essentially ruled out by the UFB-3 constraint for the heterotic string scale [25].

5 SUGRA scenario with non-universal soft terms

As mentioned in the Introduction, the general situation for the soft parameters is to have a non-universal structure, and in fact, generic string constructions, whose low-energy limit is SUGRA, exhibit these properties. It was shown in the literature that the non-universality of the soft parameters allows to increase the neutralino-proton cross section. This can be carried out with non-universal scalar masses [57, 58, 13, 62, 12, 15, 18] and/or gaugino masses [19, 62, 15, 20, 18, 21]. We will concentrate on this possibility here, taking into account the effect of the charge and colour breaking constraints.

(i) Non-universal scalar masses

Let us analyse for the moment a SUGRA scenario with GUT scale and non-universal soft scalar masses. This non-universality can be parameterized in the Higgs sector as follows:

$$m^2_{H_d} = m^2(1+\delta_1) \ , \quad m^2_{H_u} = m^2(1+\delta_2) \ . \tag{6}$$

Concerning squarks and sleptons, in order to avoid potential problems with flavour changing neutral currents, one can assume that the first two generations have a common scalar mass m at M_{GUT}, and that non-universalities are allowed only for the third generation:

$$\begin{aligned} m^2_{Q_L} &= m^2(1+\delta_3) \ , \quad m^2_{u_R} = m^2(1+\delta_4) \ , \\ m^2_{e_R} &= m^2(1+\delta_5) \ , \quad m^2_{d_R} = m^2(1+\delta_6) \ , \\ m^2_{L_L} &= m^2(1+\delta_7) \ , \end{aligned} \tag{7}$$

where $Q_L = (\tilde{t}_L, \tilde{b}_L)$, $L_L = (\tilde{\nu}_L, \tilde{\tau}_L)$, $u_R = \tilde{t}_R$ and $e_R = \tilde{\tau}_R$. Note that whereas $\delta_i \geq -1$, $i = 3, ..., 7$, in order to avoid an UFB direction breaking charge and colour, $\delta_{1,2} \leq -1$ is possible as long as the conditions $m_1^2 = m^2_{H_d} + \mu^2 > 0$, $m_2^2 = m^2_{H_u} + \mu^2 > 0$ are fulfiled.

As discussed for intermediate scales in Subsection 4.2, an important factor in order to increase the cross section, consists in reducing the value of $|\mu|$. This value is determined by condition (1) and can be significantly reduced for some choices of the δ's. We can have a qualitative understanding of the effects of the δ's on μ from the following. First, when $m^2_{H_u}$ at M_{GUT} increases its negative low-energy contribution to eq. (1) becomes less important. Second, when $m^2_{Q_L}$ and $m^2_{u_R}$ at M_{GUT} decrease, due to their contribution proportional to the top Yukawa coupling in the RGE of $m^2_{H_u}$, the negative contribution of the latter to μ^2 is again less important. Thus one can deduce that μ^2 will be reduced (and hence $\sigma_{\tilde{\chi}^0_1 - p}$ increased) by choosing $\delta_{3,4} < 0$ and $\delta_2 > 0$. In fact non-universalities in the Higgs sector give the most important effect, and including the one in the sfermion sector the cross section only increases slightly. Thus in what follows we will take $\delta_i = 0$, $i = 3, ..., 7$.

Concerning the value of the relic density, $\Omega_{\tilde{\chi}^0_1}$ is affected due to the increase of the Higgsino components of $\tilde{\chi}^0_1$ with respect to the dominant bino component of the universal case. The change in μ also determines the presence of the Higgs mediated resonant

channels. In contrast to Subsection 4.2, the most relevant coannihilation scenarios are $\tilde{\chi}_1^0$–$\tilde{\tau}_1$, in particular $\tilde{\chi}_1^0$–$\tilde{\chi}_1^\pm$ coannihilations are only sizeable for $\tan\beta = 35$ in Fig. 12 (see the discussion below), when the μ–parameter becomes small. However, even in this case the area inside the WMAP bounds corresponds to neutralino annihilations, which are enhanced due to enlargement of its Higgsino components.

On the other hand, there is another relevant way of increasing the cross section using the non-universalities of the Higgs sector. Note that decreasing $m_{H_d}^2$, i.e. choosing $\delta_1 < 0$, leads to a decrease in $m_A^2 = m_{H_d}^2 + m_{H_u}^2 + 2\mu^2$ and therefore in the mass of the heaviest Higgs[3] H. This produces an increase in the cross section.

Thus we will see that, unlike the universal scenario in Section 4, with non-universalities is possible to obtain large values of the cross section, and even some points enter in the DAMA area fulfilling all constraints. Let us analyse three representative cases with

$$\begin{aligned} a)\ \delta_1 &= 0 \quad , \quad \delta_2 = 1 \ , \\ b)\ \delta_1 &= -1 \quad , \quad \delta_2 = 0 \ , \\ c)\ \delta_1 &= -1 \quad , \quad \delta_2 = 1 \ . \end{aligned} \tag{8}$$

Clearly, the above discussion about decreasing μ^2 applies well to case *a)*, where the variation in $m_{H_u}^2$ through δ_2 is relevant. This is shown in Fig. 12 for $\tan\beta = 35, 50$ and $A = 0$, which can be compared with Figs. 2 and 3. Note that now, for $\tan\beta = 35$, there is an important area in the upper left where μ^2 becomes negative due to the increasing in δ_2 with respect to the universal case. A larger area is forbidden for large values of $\tan\beta$, as e.g. $\tan\beta = 50$, but now because m_A^2 becomes negative. This is similar to what occurs in the universal scenario when $\tan\beta \gtrsim 60$, as mentioned in Section 3. Notice that eq. (1) can be written as $\mu^2 \approx -m_{H_u}^2 - \frac{1}{2}M_Z^2$ and therefore $m_A^2 \approx m_{H_d}^2 - m_{H_u}^2 - M_Z^2$. Since $m_{H_u}^2$ at M_{GUT} increases its negative low-energy contribution becomes less important. In addition, the bottom Yukawa coupling is large and the $m_{H_d}^2$ becomes negative. As a consequence $m_A^2 < 0$.

For $\tan\beta = 35$, although the cross section increases with respect to the universal case, the present experimental constraints exclude points entering in the DAMA area. This can be seen more clearly comparing Figs. 13 and 4. Notice also that the astrophysical bounds $0.1 \lesssim \Omega_{\tilde{\chi}_1^0} h^2 \lesssim 0.3$ imply $\sigma_{\tilde{\chi}_1^0 - p} \approx 10^{-8}$ pb. On the contrary, for $\tan\beta = 50$ there are points entering in the DAMA area, and even part of them fulfil the astrophysical bounds. We have checked that for $A = M$ the figures are similar, although no points enter in the DAMA area, even for $\tan\beta = 50$. On the other hand, the region forbidden by the LSP bound is larger than the one forbidden by the UFB-3 constraint.

We have also checked that larger values of δ_2, as e.g. $\delta_2 = 1.5$, give rise to similar figures. For small values, $\delta_2 \gtrsim 0.2$ is sufficient to enter in DAMA fulfilling the experimental bounds with $\tan\beta = 50$. In fact, e.g., for $\delta_2 = 0.5, 0.75$ one also gets many points entering in DAMA as for $\delta_2 = 1$, however, they do not fulfil the astrophysical bounds. For the latter one needs $\delta_2 > 0.85$.

[3]On the contrary, the lightest Higgs mass, m_h, is almost unaltered, it only decreases less than 1%.

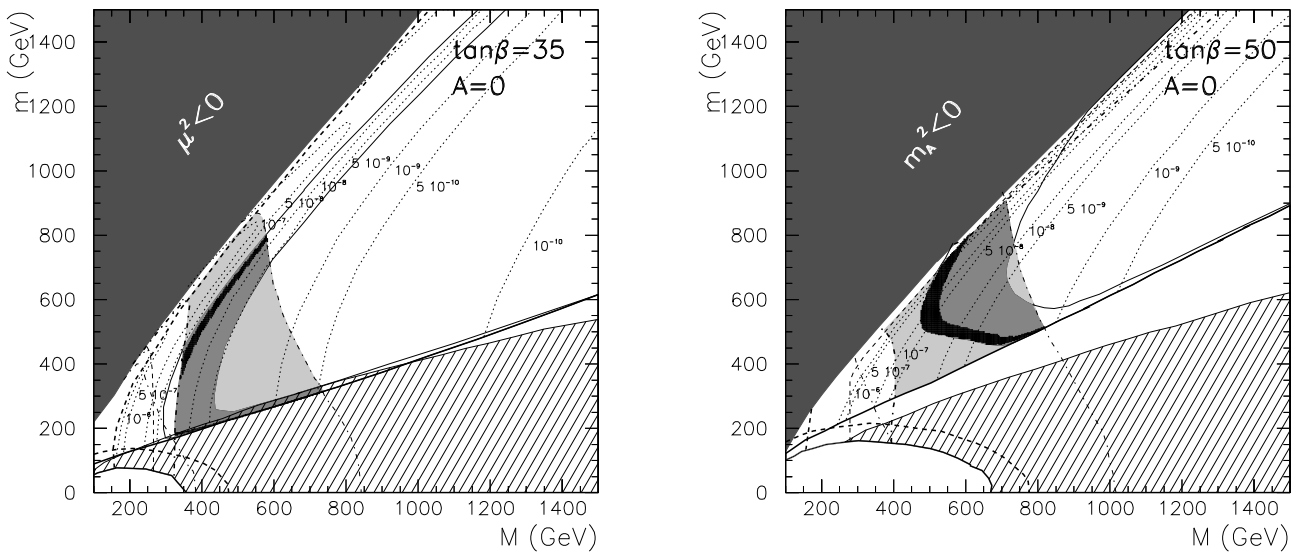

Figure 12: The same as in Figs. 2 and 3 but for the non-universal case *a)* $\delta_1 = 0$, $\delta_2 = 1$, discussed in eq. (8), with $\tan\beta = 35, 50$ and $A = 0$.

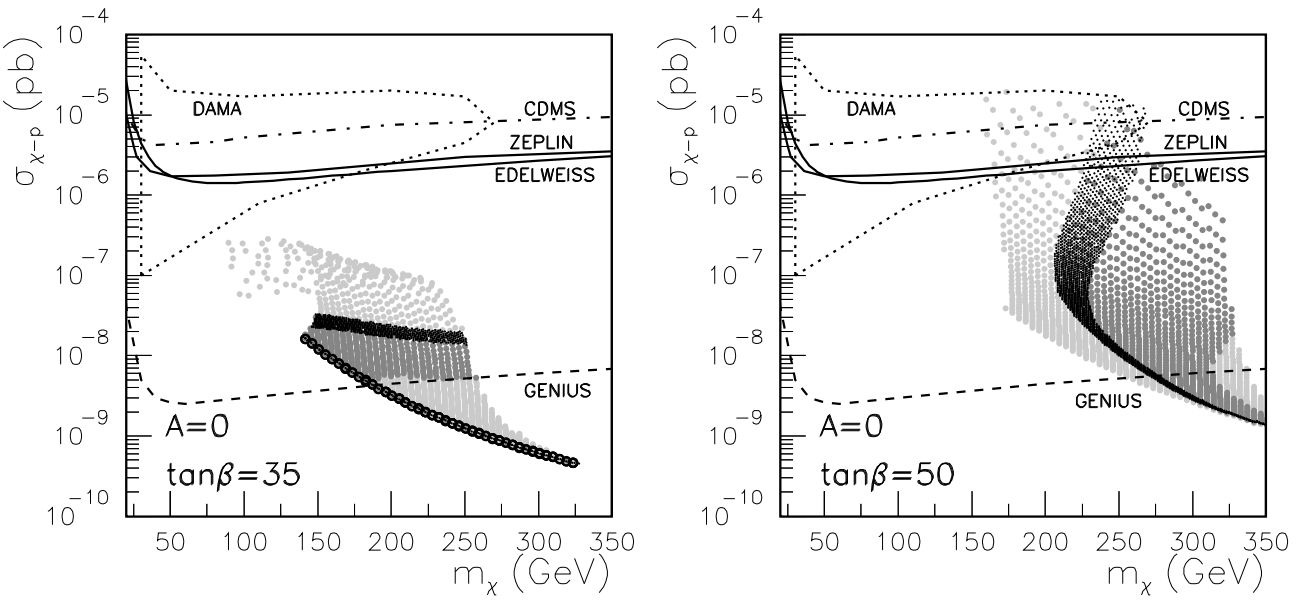

Figure 13: The same as in Figs. 4 and 5 but for the non-universal case *a)* $\delta_1 = 0$, $\delta_2 = 1$, discussed in eq. (8), with $\tan\beta = 35, 50$ and $A = 0$.

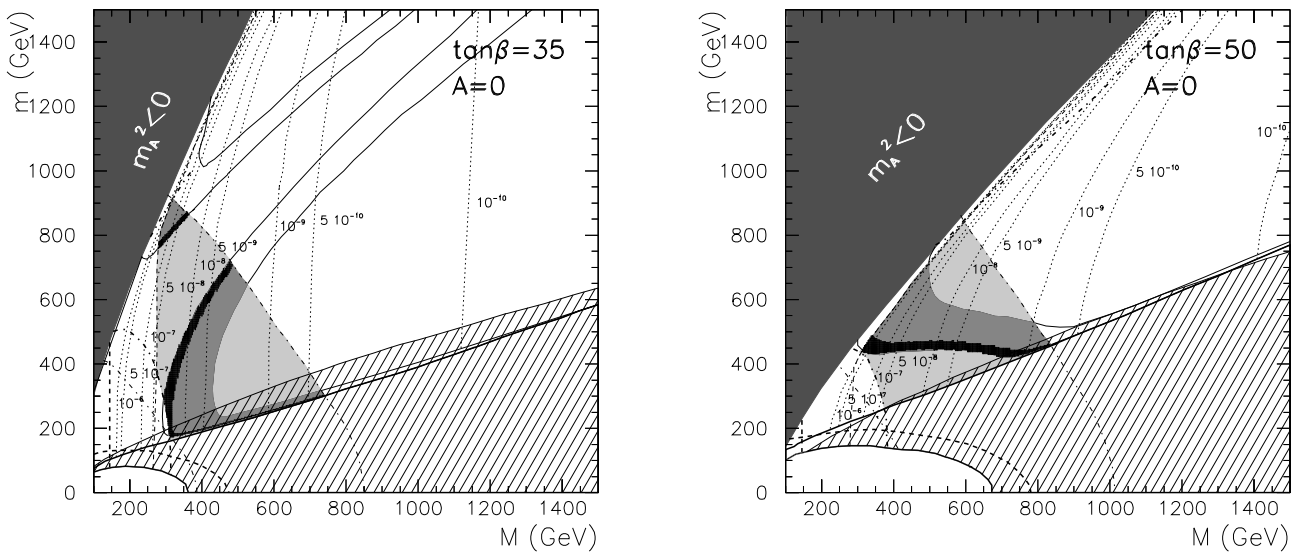

Figure 14: The same as in Figs. 2 and 3 but for the non-universal case *b)* $\delta_1 = -1$, $\delta_2 = 0$, discussed in eq. (8), with $\tan\beta = 35, 50$ and $A = 0$.

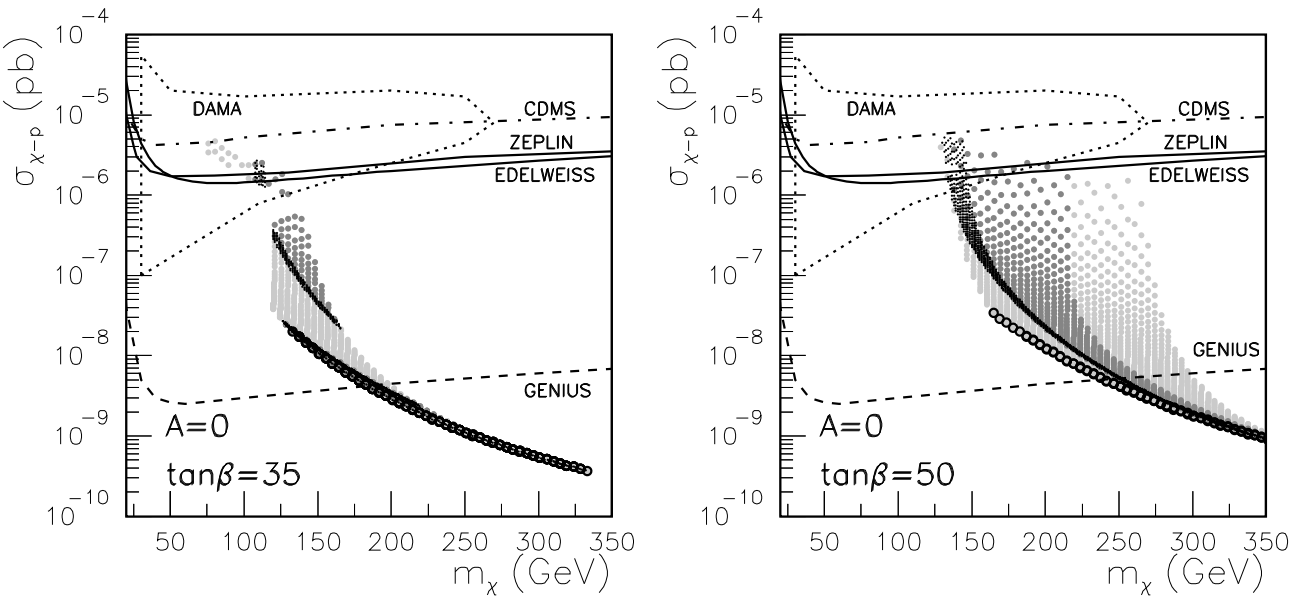

Figure 15: The same as in Figs. 4 and 5 but for the non-universal case *b)* $\delta_1 = -1$, $\delta_2 = 0$, discussed in eq. (8), with $\tan\beta = 35, 50$ and $A = 0$.

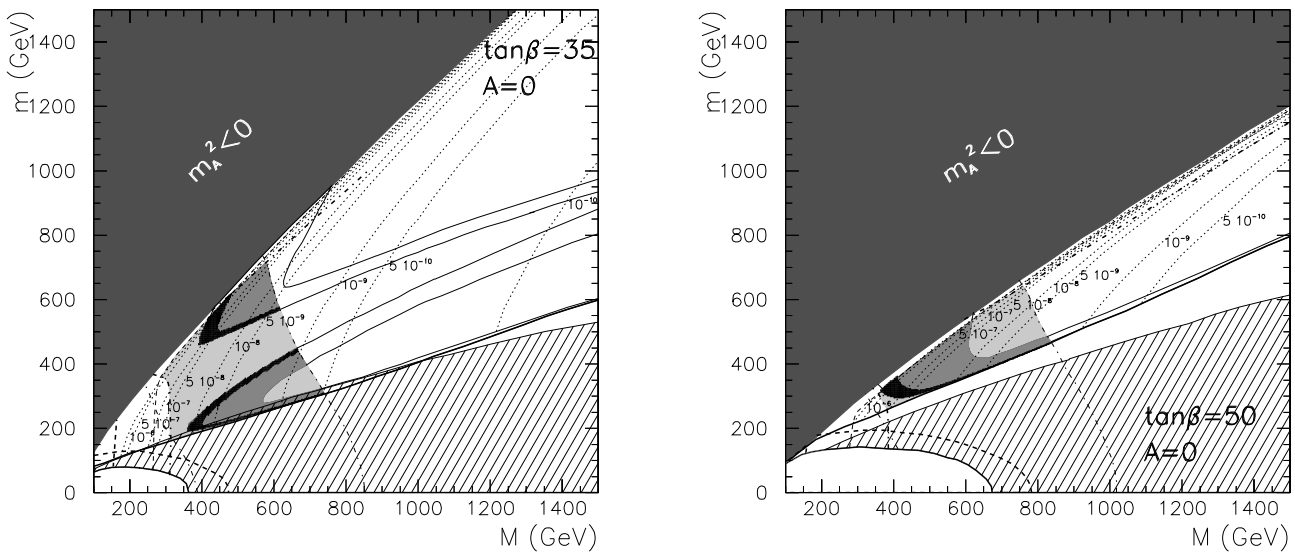

Figure 16: The same as in Figs. 2 and 3 but for the non-universal case *c)* $\delta_1 = -1$, $\delta_2 = 1$, discussed in eq. (8), with $\tan\beta = 35, 50$ and $A = 0$.

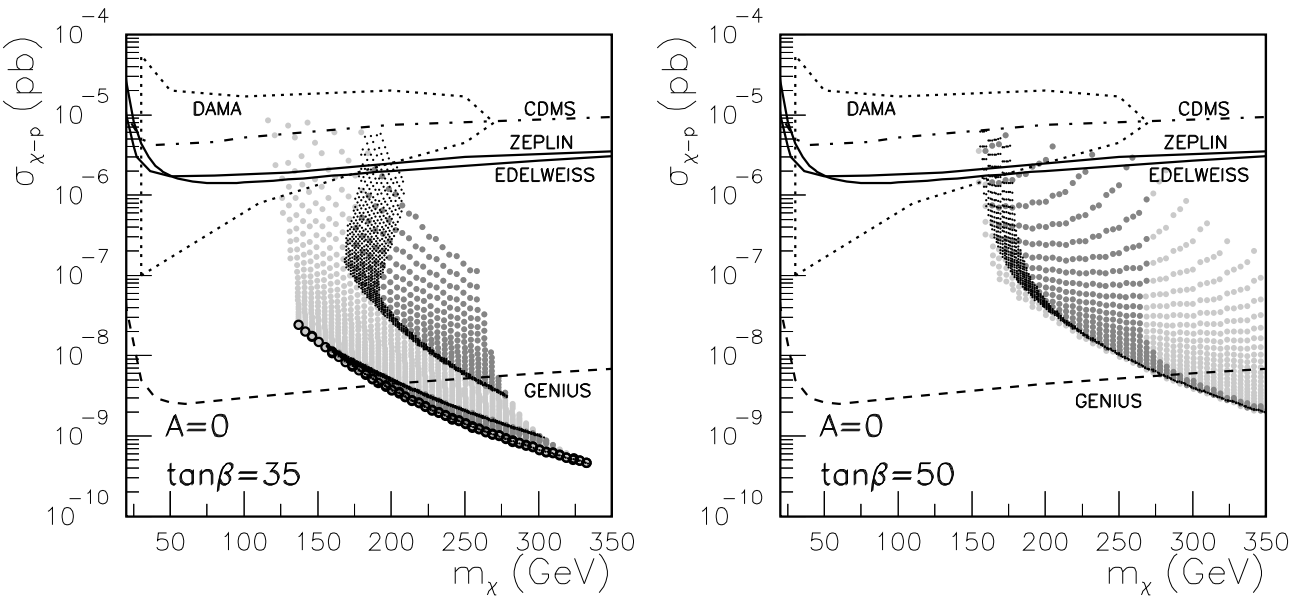

Figure 17: The same as in Figs. 4 and 5 but for the non-universal case *c)* $\delta_1 = -1$, $\delta_2 = 1$, discussed in eq. (8), with $\tan\beta = 35, 50$ and $A = 0$.

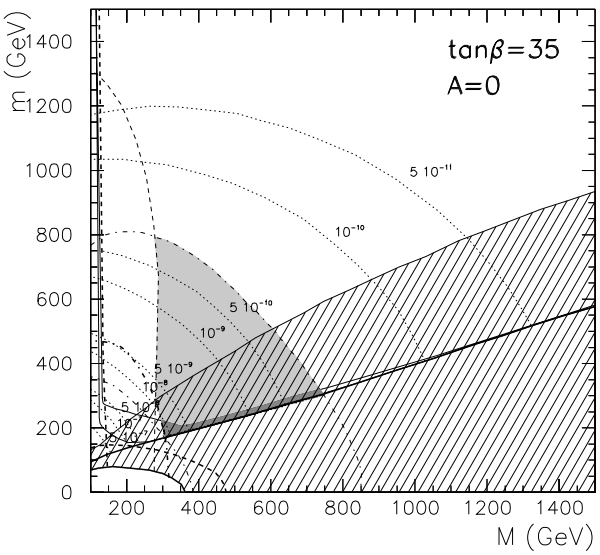

Figure 18: The same as in Fig. 12 but for $\delta_1 = 0$, $\delta_2 = -1$, with $\tan\beta = 35$ and $A = 0$.

Let us finally remark that although $\sin^2(\alpha - \beta)$ is close to 1 in most of the points, a small number of them can have smaller values when $\tan\beta = 50$. These are points close to the region with $m_A^2 < 0$, and therefore with small values for m_A. The same situation occurs for the other cases studied below. Thus, according to our discussion in Section 3, we use for these points the appropriate bound on the Higgs mass [34]. In particular, in Fig. 13, the light grey dots above the CDMS line correspond to these points.

For case *b)* the cross section increases also substantially with respect to the universal case. Now δ_2 is taken vanishing and therefore the value of μ is essentially not modified with respect to the universal case. However, taking $\delta_1 = -1$ produces an increase in the cross section through the decrease in m_A^2, as discussed previously. Note that for this case there is an area in the upper left of Fig. 14 where m_A^2 becomes negative. As shown explicitly in Fig. 15, for $\tan\beta = 35$ and $A = 0$, there are points in the DAMA region. All of them correspond to $\sin^2(\alpha - \beta)$ not close to 1, and therefore with an experimental bound on the Higgs mass smaller than 114.1 GeV. All points with $\sin^2(\alpha - \beta) \sim 1$ have $\sigma_{\tilde{\chi}_1^0 - p} \lesssim 6 \times 10^{-7}$ pb. Note that points with large values of the cross section fulfil in this case the astrophysical bound $\Omega_{\tilde{\chi}_1^0} h^2 \gtrsim 0.1$. Large values of m reduce the resonant effects produced by the Higgs A, and are sufficient to place the relic abundance inside the bounds. For $\tan\beta = 50$, similarly to case *a)*, there are points entering in the DAMA area, and part of them fulfil the astrophysical bounds. Those above the ZEPLIN line correspond to $\sin^2(\alpha - \beta)$ not close to 1. For $A = M$ the figures as similar.

We have checked that smaller values of δ_1, as e.g. $\delta_1 = -1.5, -2$, give also rise to

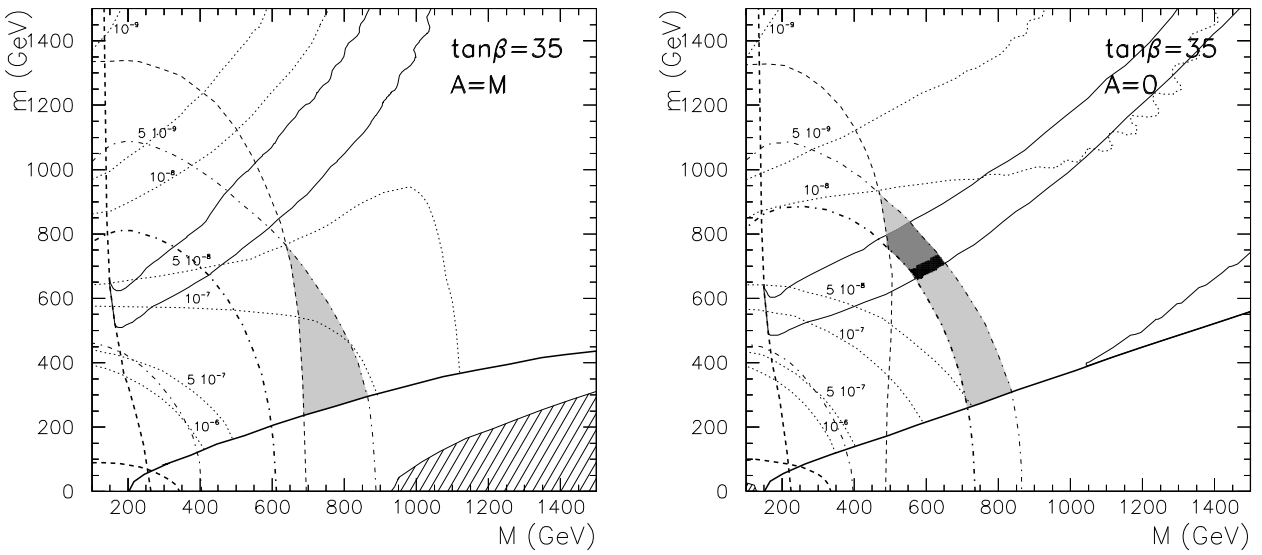

Figure 19: The same as in Fig. 2 but for the case discussed in eq. (9) with non-universal soft gaugino masses, $\delta'_{1,2} = 0, \delta'_3 = -0.5$, taking $\tan\beta = 35$ and $A = M, 0$.

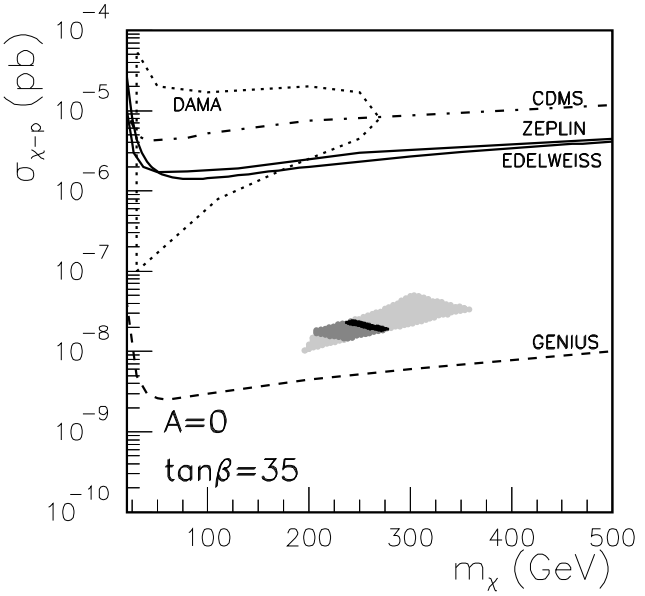

Figure 20: The same as in Fig. 4 but for the case discussed in eq. (9) with non-universal soft gaugino masses, $\delta'_{1,2} = 0, \delta'_3 = -0.5$, taking $\tan\beta = 35$ and $A = 0$.

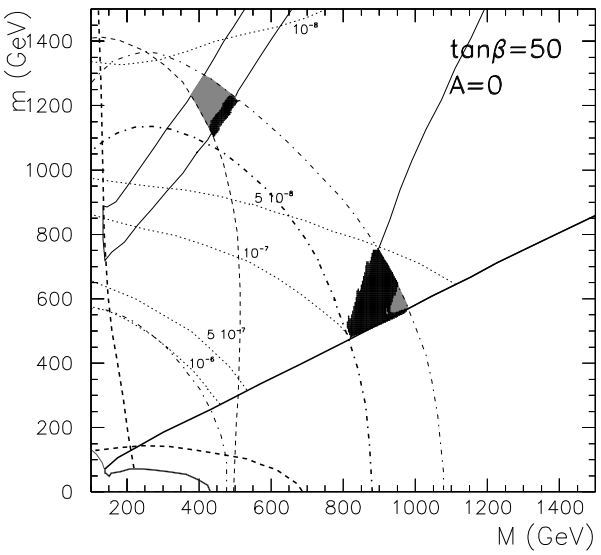

Figure 21: The same as in Fig. 19 but for $\tan\beta = 50$ and $A = 0$.

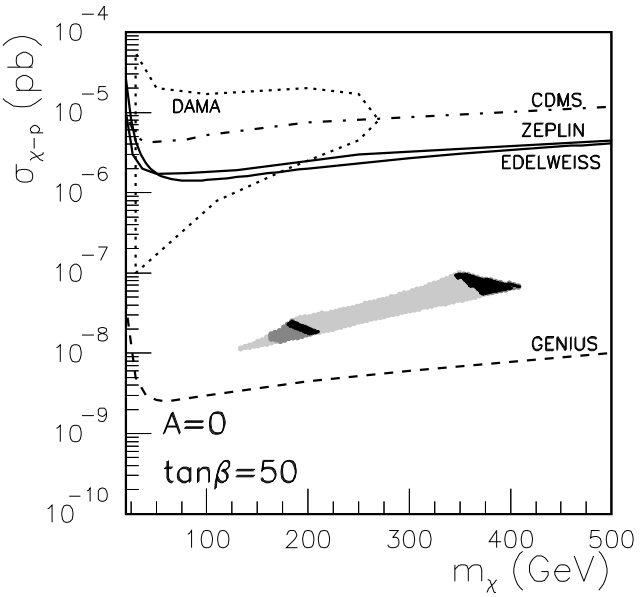

Figure 22: The same as in Fig. 20 but for $\tan\beta = 50$ and $A = 0$.

similar figures. For larger values, $\delta_1 \lesssim -0.4$ is sufficient to enter in DAMA fulfilling the experimental and astrophysical bounds with $\tan\beta = 50$.

Finally, given the above situation concerning the enhancement of the neutralino-proton cross section for *a)* and *b)*, it is clear that the combination of both cases might be interesting. This is carried out in case *c)* where we take $\delta_1 = -1$ and $\delta_2 = 1$. As shown in Figs. 16 and 17, cross sections as large as $\sigma_{\tilde{\chi}^0_1-p} \gtrsim 10^{-6}$ pb, entering in DAMA and fulfilling all experimental and astrophysical bounds, can be obtained for $\tan\beta = 35, 50$ and $A = 0$. Those above the ZEPLIN line correspond to $\sin^2(\alpha-\beta)$ not close to 1. On the other hand, for $A = M$ and $\tan\beta = 35$ no points with the correct relic density enter in DAMA. For other cases the results are similar. For example, if we consider $\delta_1 = -0.5$ and $\delta_2 = 1$, one obtains for $\tan\beta = 35$ points entering in DAMA but with $\Omega_{\tilde{\chi}^0_1}h^2 < 0.01$. For $\tan\beta = 50$ a similar plot to the one in Fig. 17 is obtained.

Concerning the restrictions coming from the UFB-3 constraint, we can see in Figs. 12, 14 and 16 that these are slightly less important than in the universal scenario (see Figs. 2 and 3). For example, for case *a)*, as in the intermediate scale case, the main reason is that $m^2_{H_u}$ at low energy becomes less negative. Thus the value of V_{UFB-3} is increased, making the UFB-3 constraint less restrictive. For comparison, we show in Fig. 18 the same case as in Fig. 12, for $\tan\beta = 35$, but using the opposite choice for the sign of the δ parameters. Not only the cross section is smaller, $\sigma_{\tilde{\chi}^0_1-p} < 10^{-8}$ pb, but also the UFB-3 constraint is very restrictive, forbidding all points which are allowed by the experimental and astrophysical constraints.

(ii) Non-universal gaugino masses

Concerning gaugino masses, let us parameterize their non-universality at M_{GUT} as follows:

$$M_1 = M(1+\delta'_1)\ , \quad M_2 = M(1+\delta'_2)\ , \quad M_3 = M(1+\delta'_3)\ , \tag{9}$$

where $M_{1,2,3}$ are the bino, wino and gluino masses, respectively. Let us discuss now which values of the parameters are interesting in order to increase the cross section with respect to the universal case $\delta'_i = 0$. In this sense, it is worth noticing that M_3 appears in the RGEs of squark masses, so e.g. their contribution proportional to the top Yukawa coupling in the RGE of $m^2_{H_u}$ will do this less negative if M_3 is small, and therefore μ^2 will become smaller in this case. However, small values of M_3 also lead to an important decrease in the Higgs mass[4]. In addition, $b \to s\gamma$ and $g_\mu - 2$ constraints are also relevant. We show this in Fig. 19 for $\tan\beta = 35$ and $A = M, 0$, using $\delta'_{1,2} = 0, \delta'_3 = -0.5$. As can be seen in the figure, although the cross section increases with respect to the universal case, the present experimental constraints exclude points entering in the DAMA region. On the other hand, only for $A = 0$ there are points allowed by all experimental and astrophysical constraints, and they correspond to $\sigma_{\tilde{\chi}^0_1-p} \approx 3\times 10^{-8}$ pb. Note that in this case $\Omega_{\tilde{\chi}^0_1}h^2$ decreases with respect to the universal case due to the enhancement of wino

[4]We have checked that generically the value of $\sin^2(\alpha-\beta)$ is very close to 1, and therefore we are using the lower bound $m_h = 114.1$ GeV as in the mSUGRA scenario.

and Higgsino components of the $\tilde{\chi}_1^0$. The corresponding increase of the annihilation cross section makes possible the existence of the bands displayed in the figure without appealing to any kind of coannihilations. The result concerning the cross section is summarized in Fig. 20. Other values of δ's lead to qualitatively similar results. For $\tan\beta = 50$ the situation is similar, and we show the case $A = 0$ in Figs. 21 and 22.

Finally, as in the previous case with non-universal scalars, increasing the cross section through values at low energy of $m_{H_u}^2$ less negatives implies less important UFB constraints. Now these are not very relevant, and in fact they correspond to the UFB-1 ones.

6 Conclusions

We have carried out a theoretical analysis of the possibility of detecting dark matter directly in current and projected experiments. In particular, we have studied the value of the neutralino-nucleon cross section in several supergravity scenarios. In addition to the usual experimental and astrophysical constraints we have imposed on the parameter space the absence of dangerous charge and colour breaking minima. This constraint, in particular the UFB-3, turns out to be quite important in some cases. For example, in the usual mSUGRA scenario, where the soft terms are assumed to be universal, and the GUT scale is considered, $\tan\beta \lesssim 20$ is forbidden on this ground. In fact, even larger values of $\tan\beta$ can also be forbidden, depending on the value of the trilinear parameter A. Concerning the cross section, this is constrained to be $\sigma_{\tilde{\chi}_1^0-p} \lesssim 3\times 10^{-8}$ pb, and therefore below the DAMA-reported data. Obviously, more sensitive detectors, as e.g. GENIUS where values of the cross section as low as 10^{-9} pb will be accessible, are needed.

When an intermediate scale is considered, the running of the parameters is shorter, and in particular $m_{H_u}^2$ is less negative at low energy producing a decrease in the value of μ^2. Although this effect increases the cross section, it is not sufficient yet to enter in the DAMA area because of the experimental bounds, which impose $\sigma_{\tilde{\chi}_1^0-p} \lesssim 4\times 10^{-7}$ pb. In fact, at the end of the day, the preferred astrophysical range for the relic neutralino density, $0.1 \leq \Omega_{\tilde{\chi}_1^0} h^2 \leq 0.3$, imposes $\sigma_{\tilde{\chi}_1^0-p} \lesssim 10^{-7}$ pb. On the other hand, when $m_{H_u}^2$ is less negative the negative contribution to V_{UFB-3} is less important, and therefore also is less important the UFB-3 constraint. In fact, values of $\tan\beta$ smaller than 20 are now allowed.

A similar situation concerning the UFB-3 constraint occurs when non-universal soft terms are allowed and we try to increase the cross section, since this is carried out by imposing a less negative value of $m_{H_u}^2$ at low energy. As a consequence the UFB-3 constraint is slightly less important than in the universal scenario. The other possibility to achieve this, to decrease $m_{H_d}^2$, does not modify essentially the UFB-3 constraint. Of course, if the opposite procedure is carried out, choosing the parameters in such a way that the cross section decreases, the UFB-3 constraint is more important.

Concerning the cross section, this can be increased a lot with respect to the universal scenario, when non-universal scalars are considered. It is even possible, for some

particular values of the parameters, to find points entering in DAMA, $\sigma_{\tilde{\chi}_1^0-p} \approx 10^{-6}$ pb, and fulfilling all experimental and astrophysical constraints. On the contrary, when non-universal gauginos are considered, although the cross section increases, the experimental bounds exclude the possibility of entering in DAMA.

Acknowledgements
The work of D.G. Cerdeño was supported by the Deutsche Forschungsgemeinschaft. D.G. Cerdeño also thanks the MLU Halle-Wittenberg for their hospitality during the early stages of this work. E. Gabrielli would like to thank the Academy of Finland (project number 48787) for financial support. M.E. Gomez acknowledges support from the Fundação para a Ciência e Tecnologia under contract SFRH/BPD/5711/2001 and project CFIF-Plurianual (2/91). The work of C. Muñoz was supported in part by the Ministerio de Ciencia y Tecnología under contract FPA2000-0980, and the European Union under contract HPRN-CT-2000-00148.

References

[1] For a recent review see e.g., S. Khalil and C. Muñoz, Contemp. Phys. 43 (2002) 51 [hep-ph/0110122].

[2] DAMA Collaboration, R. Bernabei et al., Phys. Lett. B480 (2000) 23.

[3] P. Belli, R. Cerulli, N. Fornengo and S. Scopel, Phys. Rev. D66 (2002) 043503.

[4] CDMS Collaboration, R. Abusaidi et al., Phys. Rev. Lett. 84 (2000) 5699; Phys. Rev. D66 (2002) 122003.

[5] EDELWEISS Collaboration, A. Benoit et al., Phys. Lett. B513 (2001) 15; ibid. B545 (2002) 43.

[6] IGEX Collaboration, A. Morales et al., Phys. Lett. B532 (2002) 8.

[7] ZEPLIN I Collaboration, N.J.T. Smith et al., talk given at the 4th International Workshop idm2002, York, England.

[8] M. Drees and M.M. Nojiri, Phys. Rev. D45 (1992) 2482.

[9] G. Gamberini, G. Ridolfi and F. Zwirner, in ref. [23].

[10] For a review see, A. Brignole, L.E. Ibanez and C. Muñoz, in the book 'Perspectives on Supersymmetry', Ed. G. Kane, World Scientific (1998) 125 [hep-ph/9707209].

[11] J. Ellis, A. Ferstl and K.A. Olive, Phys. Lett. B532 (2002) 318.

[12] J. Ellis, K.A. Olive and Y. Santoso Phys. Lett. B539 (2002) 107; J. Ellis, T. Falk, K.A. Olive and Y. Santoso, Nucl. Phys. B652 (2003) 259; J. Ellis, A. Ferstl, K.A. Olive and Y. Santoso, hep-ph/0302032.

[13] M. Drees, Y.G. Kim, T. Kobayashi and M.M. Nojiri, Phys. Rev. D63 (2001) 115009.

[14] M.E. Gomez and J.D. Vergados, Phys. Lett. B512 (2001) 252; ibid. hep-ph/0105115.

[15] D.G. Cerdeño, E. Gabrielli and C. Muñoz, Proceedings of Corfu Summer Institute on Elementary Particle Physics (2001) [hep-ph/0204271].

[16] A.B. Lahanas, D.V. Nanopoulos and V.C. Spanos, hep-ph/0205225.

[17] Y.G. Kim, T. Nihei, L. Roszkowski and R. Ruiz de Austri, JHEP 0212 (2002) 034.

[18] R. Arnowitt and B. Dutta, hep-ph/0210339.

[19] A. Corsetti and P. Nath, Phys. Rev. D64 (2001) 125010.

[20] V. Bertin, E. Nezri and J. Orloff, JHEP 0302 (2003) 046.

[21] A. Birkedal-Hansen and B.D. Nelson, Phys. Rev. D67 (2003) 095006.

[22] For a review see e.g., C. Muñoz, hep-ph/9709329.

[23] J.M. Frere, D.R.T. Jones and S. Raby, Nucl. Phys. B222 (1983) 11; L. Alvarez-Gaumé, J. Polchinski and M. Wise, Nucl. Phys. B221 (1983) 495; J.P. Derendinger and C.A. Savoy, Nucl. Phys. B237 (1984) 307; C. Kounnas, A.B. Lahanas, D.V. Nanopoulos and M. Quirós, Nucl. Phys. B236 (1984) 438; M. Drees, M. Glück and K. Grassie, Phys. Lett. B157 (1985) 164; J.F. Gunion, H.E. Haber and M. Sher, Nucl. Phys. B306 (1988) 1; H. Komatsu, Phys. Lett. B215 (1988) 323; G. Gamberini, G. Ridolfi and F. Zwirner, Nucl. Phys. B331 (1990) 331; P. Langacker and N. Polonsky, Phys. Rev. D50 (1994) 2199.

[24] J.A. Casas, A. Lleyda and C. Muñoz, Nucl. Phys. B471 (1996) 3.

[25] J.A. Casas, A. Lleyda and C. Muñoz, Phys. Lett. B380 (1996) 59.

[26] J.A. Casas, A. Lleyda and C. Muñoz, Phys. Lett. B389 (1996) 305.

[27] J.A. Casas and S. Dimopoulos, Phys. Lett. B387 (1996) 107; H. Baer, M. Bhrlik and D. Castaño, Phys. Rev. D54 (1996) 6944; S.A. Abel and B.C. Allanach, Phys. Lett. B415 (1997) 371; ibid. B431 (1998) 339; S.A. Abel and T. Falk, Phys. Lett. B444 (1998) 427.

[28] J.A. Casas, A. Ibarra and C. Muñoz, Nucl. Phys. B554 (1999) 67.

[29] S.A. Abel, B.C. Allanach, F. Quevedo, L.E. Ibáñez and M. Klein, JHEP 0012 (2000) 026.

[30] E. Gabrielli, K. Huitu and S. Roy, Phys. Rev. D65 (2002) 075005.

[31] M. Claudson, L.J. Hall and I. Hinchliffe, Nucl. Phys. B228 (1983) 501; T. Falk, K. Olive, L. Roszkowski and M. Srednicki, Phys. Lett. B367 (1996) 183; A. Riotto and E. Roulet, Phys. Lett. B377 (1996) 60; A. Kusenko, P. Langacker and G. Segre, Phys. Rev. D54 (1996) 5824; A. Strumia, Nucl. Phys. B482 (1996) 24; A. Kusenko and P. Langacker, Phys. Lett. B391 (1997) 29; T. Falk, K.A. Olive, L. Roszkowski, A. Singh and M. Srednicki, Phys. Lett. B396 (1997) 50; S.A. Abel and C.A. Savoy, Nucl. Phys. B532 (1998) 3; I. Dasgupta, R. Rademacher and P. Suranyi, Phys. Lett. B447 (1999) 284.

[32] S. Ambrosiano, A. Dedes, S. Heinemeyer, S. Su and G. Weiglein, Nucl. Phys. B624 (2002) 3.

[33] J.F. Gunion and H.E. Haber, Nucl. Phys. B272 (1986) 1; ibid. B278 (1986) 449; ibid. B307 (1988) 445; Erratum-ibid. B402 (1993) 567; A. Djouadi, J. Kalinowski and P.M. Zerwas, Z. Phys. C57 (1993) 569.

[34] ALEPH Collaboration, R. Barate et al., Phys. Lett. B499 (2001) 53.

[35] S. Heinemeyer, W. Hollik and G. Weiglein, Comp. Phys. Comm. 124 (2000) 76; hep-ph/0002213; M. Frank, S. Heinemeyer, W. Hollik and G. Weiglein, hep-ph/0202166.

[36] G. Rodrigo and A. Santamaria, Phys. Lett. B313 (1993) 441; G. Rodrigo, A. Pich and A. Santamaria, Phys. Lett. B424 (1998) 367; H. Baer, J. Ferrandis, K. Melnikov and X. Tata, Phys. Rev. D66 (2002) 074007.

[37] L.J. Hall, R. Rattazzi and U. Sarid, Phys. Rev. D50 (1994) 7048; M. Carena, S. Pokorski, M. Olechowski and C.E.M. Wagner, Nucl. Phys. B426 (1994) 269; D.M. Pierce, J.A. Bagger, K.T. Matchev and R.-J. Zhang, Nucl. Phys. B491 (1997) 3.

[38] Joint LEP 2 supersymmetry working group, http://lepsusy.web.cern.ch/lepsusy /www/inos_moriond01/ charginos_pub.html

[39] Joint LEP 2 supersymmetry working group, http://alephwww.cern.ch/~ganis /SUSYWG/SLEP/sleptons_2k01.html

[40] CLEO Collaboration, S. Chen et al., Phys. Rev. Lett. 87 (2001) 251807.

[41] BELLE Collaboration, H. Tajima, Int. J. Mod. Phys. A17 (2002) 2967.

[42] G. Belanger, F. Boudjema, A. Pukhov and A. Semenov, Comput. Phys. Commun. 149 (2002) 103; hep-ph/0210327; G. Belanger, hep-ph/0210350.

[43] M.E. Gomez, G. Lazarides and C. Pallis, hep-ph/0301064.

[44] G. D'Ambrosio, G.F. Giudice, G. Isidori, A. Strumia, Nucl. Phys. B645 (2002) 155.

[45] Muon $g-2$ Collaboration, G.W. Bennet et al., Phys. Rev. Lett. 89 (2002) 101804; Erratum-ibid. 89 (2002) 129903.

[46] M. Davier, S. Eidelman, A. Hocker and Z. Zhang, hep-ph/0208177; K. Hagiwara, A.D. Martin, D. Nomura and T. Teubner, hep-ph/0209187.

[47] See, e.g., A. Kudo and M. Yamaguchi, Phys. Lett. B516 (2001) 151, and references therein.

[48] C.L. Bennett et al., astro-ph/0302207; D.N. Spergel et al., astro-ph/0302209.

[49] See e.g., S. Khalil, C. Muñoz and E. Torrente-Lujan, New J. Phys. 4 (2002) 27, and references therein.

[50] For a review see e.g., G. Jungman, M. Kamionkowski and K. Griest, Phys. Rept. 267 (1996) 195.

[51] J. R. Ellis, T. Falk and K. A. Olive, Phys. Lett. B 444 (1998) 367; J. R. Ellis, T. Falk, K. A. Olive and M. Srednicki, Astropart. Phys. 13 (2000) 181 [Erratum-ibid. 15 (2001) 413]; M. E. Gomez, G. Lazarides and C. Pallis, Phys. Rev. D 61 (2000) 123512, Phys. Lett. B 487 (2000) 313; A. B. Lahanas, D. V. Nanopoulos and V. C. Spanos, Phys. Rev. D 62 (2000) 023515; J. R. Ellis, T. Falk, G. Ganis, K. A. Olive and M. Srednicki, Phys. Lett. B 510 (2001) 236; T. Nihei, L. Roszkowski and R. Ruiz de Austri, JHEP 0207 (2002) 024; J. R. Ellis, T. Falk, K. A. Olive and Y. Santoso, Nucl. Phys. B 652 (2003) 259.

[52] J. Edsjo and P. Gondolo, Phys. Rev. D 56 (1997) 1879; P. Gondolo, J. Edsjo, P. Ullio, L. Bergstrom, M. Schelke and E. A. Baltz, astro-ph/0211238; R. Arnowitt, B. Dutta and Y. Santoso, Nucl. Phys. B 606 (2001) 59; A. Birkedal-Hansen and B. D. Nelson, Phys. Rev. D 64 (2001) 015008; H. Baer, C. Balazs and A. Belyaev, JHEP 0203 (2002) 042; J. Edsjo, M. Schelke, P. Ullio and P. Gondolo, JCAP 0304 (2003) 001.

[53] C. Boehm, A. Djouadi and M. Drees, Phys. Rev. D 62 (2000) 035012; J. R. Ellis, K. A. Olive and Y. Santoso, Astropart. Phys. 18 (2003) 395.

[54] A. Pukhov et al., hep-ph/9908288.

[55] A. Djouadi, J. Kalinowski and M. Spira, Comput. Phys. Commun. 108 (1998) 56.

[56] M.E. Gomez, G. Lazarides and C. Pallis, Nucl. Phys. B638 (2002) 165; M.E. Gomez and C. Pallis, hep-ph/0303098.

[57] A. Bottino, F. Donato, N. Fornengo and S. Scopel, Phys. Rev. D59 (1999) 095004.

[58] E. Accomando, R. Arnowitt, B. Dutta and Y. Santoso, Nucl. Phys. B585 (2000) 124.

[59] R. Arnowitt and B. Dutta, hep-ph/0112157.

[60] H.V. Klapdor-Kleingrothaus, L. Baudis, G. Heusser, B. Majorovits and H. Paes, hep-ph/9910205.

[61] A. Bottino, F. Donato, N. Fornengo and S. Scopel, hep-ph/0208273.

[62] D.G. Cerdeño, S. Khalil and C. Muñoz, Proceedings of CICHEP Conference in Cairo, Rinton Press (2001) 214 [hep-ph/0105180].

[63] D.G. Cerdeño, E. Gabrielli, S. Khalil, C. Muñoz and E. Torrente-Lujan, Nucl. Phys. B603 (2001) 231.

[64] E. Gabrielli, S. Khalil, C. Muñoz and E. Torrente-Lujan, Phys. Rev. D63 (2001) 025008.

[65] D. Bailin, G.V. Kraniotis and A. Love, Phys. Lett. B491 (2000) 161.